Chapter 1

Advances in Void Fraction, Flow Pattern Maps and Non-Boiling Heat Transfer Two-Phase Flow in Pipes with Various Inclinations

Afshin J. Ghajar[1] and Clement C. Tang
School of Mechanical and Aerospace Engineering, Oklahoma State University, Stillwater, Oklahoma, 74078, USA

Abstract

Void fraction correlations for various pipe inclinations, both theoretical and empirical, that are widely available in the literature are compared with experimental data from various sources with different experimental facilities. The study produced a recommendation of six void fraction correlations and a proposed improved general void fraction correlation for horizontal to vertical pipe orientations. Further investigation has also been done specifically on the performances of available void fraction correlations with available experimental data for upward vertical two-phase flow. The work demonstrated that more accurate predictions can be obtained by giving attention to specific pipe inclination and ranges of void fraction. The result is a recommendation of a void fraction correlation that performs satisfactorily on the entire range of void fraction for upward vertical flow. Flow pattern maps of different pipe inclinations and gas-liquid combinations available in the literature are compared and discussed. The validity and limitations of the numerous two-phase non-boiling heat transfer correlations that have been published in the literature over the past six decades are discussed. Practical heat transfer correlations for a variety of gas-liquid flow patterns and pipe inclination angles are recommended.

Introduction

In many industrial applications, such as the flow of oil and natural gas in flow lines and wellbores, the knowledge of non-boiling two-phase, two-component (liquid and permanent gas) heat transfer is required. During the production of two-phase hydrocarbon fluids from an oil reservoir to the surface, temperature of the hydrocarbon fluids changes due to the difference in temperatures of the oil reservoir and the surface. The change in temperature results in heat transfer between the hydrocarbon fluids and the earth surrounding the oil well, and the ability to estimate the flowing temperature profile is necessary to address several design problems in petroleum production engineering [1].

In subsea oil and natural gas production, hydrocarbon fluids may leave the reservoir with a temperature of 75°C and flow in subsea surrounding of 4°C [2]. As a result of the temperature gradient between the reservoir and the surrounding, the knowledge of heat transfer is critical to prevent gas hydrate and wax deposition blockages [3]. Wax deposition can result in problems including reduction of inner pipe diameter causing

[1] E-mail address: afshin.ghajar@okstate.edu, tel: 405-744-5900, fax: 405-744-7873.

Lixin Cheng and Dieter Mewes (Ed)

blockage, increase surface roughness of pipe leading to restricted flow line pressure, decrease in production, and various mechanical problems [4]. Some examples of the economical losses caused by the wax deposition blockages include direct cost of removing the blockage from a subsea pipeline was $5 million, production downtime loss in 40 days was $25 million [5], and the cost of oil platform abandonment by Lasmo Company (U.K.) was $100 million [6].

In situations where low velocity flow is necessary while high heat transfer rates are desirable, heat transfer enhancement schemes such as coil-spring wire insert, twisted tape insert, and helical ribs are used to promote turbulence thus enhancing heat transfer. Although these heat transfer enhancement schemes have been proven to be effective, however they do come with drawbacks, such as fouling, increase in pressure drop, and sometimes even blockage. Celata *et al.* [7] presented an alternative approach to enhance heat transfer in pipe flow, by injecting gas into liquid to promote turbulence. In the experimental study performed by Celata *et al.* [7], a uniformly heated vertical pipe was internally cooled by water, while heat transfer coefficients with and without air injection were measured. The introduction of small air flow rate into the water flow resulted in increase of the heat transfer coefficient up to 20–40% for forced-convection, and even larger heat transfer enhancement for mixed-convection [7].

Two-phase flow can also occur in various situations related to ongoing and planned space operations, and the understanding of heat transfer characteristics is important for designing piping systems for space operations limited by size constraints [8]. To investigate heat transfer in two-phase slug and annular flows under reduced gravity conditions, Fore *et al.* [8, 9] conducted heat transfer measurements for air-water and air-50% aqueous glycerin abroad NASA's Zero-G KC-135 aircraft.

In the assessment of non-boiling heat transfer, void fraction and flow pattern are two critical parameters that need to be taken into consideration. In any gas-liquid system, void fraction, the volume of space occupied by gas in the system, has great effects on heat transfer, since the liquid phase generally has significantly larger thermal conductivity than the gas phase. The knowledge of flow patterns in gas-liquid system is also critical in the assessment of non-boiling heat transfer, for example heat transfer in slug flow is likely to be different than heat transfer in annular flow. Void fraction, flow pattern and heat transfer are also affected by the pipe inclination. In inclined pipes, the hydrodynamics of two-phase flow are influenced by gravitational force. The influence of gravitational force affects the slippage between the gas and liquid phases, which in turn affects the void fraction. Pipe inclination also affects the flow patterns, which is the reason behind the difference in flow pattern maps between horizontal and vertical flows. The influence of pipe inclination on the hydrodynamics of two-phase flow also leads to its effect on heat transfer. Due to the complexity and the lack of fundamental understanding of void fraction, flow patterns, and non-boiling heat transfer in two-phase flow, majority of the documented works, whether they are flow pattern maps or correlations for void fraction and heat transfer, are only applicable to selected flow conditions. Thus, the content within this chapter addresses the recent advances in void fraction, flow patterns, and non-boiling heat transfer with the effect of pipe inclination from a systematic and fundamental point of view.

Void fraction correlations for various pipe inclinations, both theoretical and empirical, that are widely available in the literature are presented. In addition, measured void fraction data from various sources and experimental facilities is also collected. The collected measured void faction data is used to validate the correlations, and a selected few correlations are recommended based on their predictive performance. In the interest of a fundamental point of view, the comparison of the measured void fraction data with the available correlations encompasses a wide range of gas and liquid flow parameters, flow patterns, and pipe inclinations for different gas-liquid combinations. Flow pattern maps for gas-liquid flow are also discussed. Flow pattern maps of different pipe inclinations and gas-liquid combinations available in the literature are compared. Since the assessment of flow patterns in a given gas-liquid system is somewhat subjective, the comparison of flow maps from various sources reveals the similarities and dissimilarities thereof. Lastly, the validity and limitations of the numerous two-phase non-boiling heat transfer correlations that have been published in the literature over the past six decades are discussed. The extensive results of the recent developments in the non-boiling two-phase heat transfer in air-water flow in horizontal and inclined pipes conducted at Oklahoma State University's two-phase flow heat transfer laboratory are presented. Practical heat transfer correlations for a variety of gas-liquid flow patterns and pipe inclination angles are recommended. The application of these correlations in engineering practice, and how they can influence the equipment design and consequently the process design are discussed.

Void Fraction in Two-Phase Pipe Flow

Comparison of void fraction correlations for different flow patterns and pipe inclinations

Due to the importance of void fraction in influencing the characteristics of two-phase flow in pipes, Woldesemayat and Ghajar [10] conducted a very extensive comparison of 68 void fraction correlations available in the open literature against 2845 experimental data points. The experimental data points were compiled from various sources with different experimental facilities [11-18]. Out of the 2845 experimental data points, 900 were for horizontal, 1542 for inclined, and 403 for vertical pipe orientations (see Table 1). Based on the comparison with experimental data, six void fraction correlations [19-24] were recommended for acceptably predicting void fraction for horizontal, upward inclined, and vertical pipe orientations regardless of flow patterns. The percentage of data points that correctly predicted the 2845 experimental data points within three error bands for each correlation is summarized in Table 2.

The three more accurate correlations out of the six correlations recommended by Woldesemayat and Ghajar [10] are developed based on drift flux model. A recent discussion on the concept of drift flux is given in [25]. Void fraction correlations based of drift flux model can be expressed generically as

$$V_{SG} = C_0 \alpha \left(V_{SG} + V_{SL} \right) + \alpha (u_{GM}) \tag{1}$$

The gas drift velocity (u_{GM}) represents the local relative velocity between gas and liquid phase. Both the two-phase distribution coefficient (C_0) and the gas drift velocity (u_{GM}) are determined empirically. In the three more accurate correlations recommended by Woldesemayat and Ghajar [10], the appropriate expressions for the two-phase distribution coefficient (C_0) and the gas drift velocity (u_{GM}) are listed in Table 3.

Table 1. Summary of experimental database sources, Woldesemayat and Ghajar [10].

Source (***no. of data points***)	**Pipe diameter [mm]** (***orientation***)	**Fluids**	**Measurement technique**
Eaton [11] (*237*)	52.5 & 102 (*H*)	Natural gas-water	Quick-closing valves
Beggs [12] (*291*)	25.4 & 38.1 (*H*, *U*, *V*)	Air-water	Quick-closing valves
Spedding & Nguyen [13] (*1383*)	45.5 (*H*, *U*, *V*)	Air-water	Quick-closing valves
Mukherjee [14] (*558*)	38.1 (*H*, *U*, *V*)	Air-kerosene	Capacitance probes
Minami & Brill [15] (*54 & 57*)	77.9 (*H*)	Air-water & Air-kerosene	Quick-closing valves
Franca & Lahey [16] (*81*)	19.0 (*H*)	Air-water	Quick-closing valves
Abdul-Majeed [17] (*83*)	50.8 (*H*)	Air-kerosene	Quick-closing valves
Sujumnong [18] (*101*)	12.7 (*V*)	Air-water	Quick-closing valves

The pipe orientations are designated with *H*, *U*, and *V* for horizontal, uphill inclined, and vertical, respectively.

Among the six void fraction correlations recommended by Woldesemayat and Ghajar [10], Dix [20] showed better performance in regards to general overall comparison with the experimental data points summarized in Table 1. The performance of the void fraction correlation by Dix [20] is shown in Fig. 1. Woldesemayat and Ghajar [10] proposed an improved void fraction correlation that gives better predictions when compared with available experimental data. The correlation proposed by Woldesemayat and Ghajar [10] was developed based on the drift flux model and takes on the following expression:

$$\alpha = \frac{V_{SG}}{C_0\left(V_{SG} + V_{SL}\right) + u_{GM}} \tag{2}$$

where the two-phase distribution coefficient (C_0) and the gas drift velocity (u_{GM}) are given as

$$C_0 = \frac{V_{SG}}{V_{SG} + V_{SL}} \left[1 + (V_{SL} / V_{SG})^{(\rho_G / \rho_L)^{0.1}} \right] \tag{2a}$$

and

$$u_{GM} = 2.9(1.22 + 1.22 \sin\theta)^{P_{atm} / P_{sys}} \left[\frac{gD\sigma(1 + \cos\theta)(\rho_L - \rho_G)}{\rho_L^2} \right]^{0.25} \tag{2b}$$

Note that the leading constant value of 2.9 in Eq. (2b) has a unit such that the drift flux velocity (u_{GM}) carries the units of meter per second, and Eq. (2) should be used with parameters conformed to the International System of Units (SI).

Table 2. Number and percentage of data points correctly predicted by the six recommended void fraction correlations and Eq. (2) for the entire experimental database summarized in Table 1, Woldesemayat and Ghajar [10].

Correlation	No. of data points within		
	±5%	±10%	±15%
Morooka *et al.* [19]	1065 (37.4%)	2137 (75.1%)	2427 (85.3%)
Dix [20]	1597 (56.1%)	2139 (75.2%)	2363 (83.1%)
Rouhani & Axelsson [21]	1082 (38.0%)	2059 (72.4%)	2395 (84.2%)
Hughmark [22]	1244 (43.7%)	2003 (70.4%)	2322 (81.6%)
Premoli *et al.* [23]	1643 (57.8%)	2084 (73.3%)	2304 (81.0%)
Filimonov *et al.* [24]	1369 (48.1%)	1953 (68.6%)	2294 (80.6%)
Woldesemayat & Ghajar [10], Eq. (2)	1718 (60.4%)	2234 (78.5%)	2436 (85.6%)

A total of 2845 experimental data points (see Table 1) were used in this comparison. The number in ( ) represents the percentage of the data points within the error band.

Table 3. Expressions for two-phase distribution coefficient (C_0) and gas drift velocity (u_{GM}) of different void fraction correlations.

Source	Two-phase distribution coefficient (C_0) and gas drift velocity (u_{GM})
Morooka *et al.* [19]	$C_0 = 1.08$ $u_{GM} = 0.45$
Dix [20]	$C_0 = \frac{V_{SG}}{V_{SG}+V_{SL}}\left[1+(V_{SL}/V_{SG})^{(\rho_G/\rho_L)^{0.1}}\right]$ $u_{GM} = 2.9\left[\frac{g\sigma(\rho_L-\rho_G)}{\rho_L^2}\right]^{0.25}$
Rouhani & Axelsson [21]	$C_0 = 1+0.2(1-x)$ $u_{GM} = 1.18(1-x)\left[\frac{g\sigma(\rho_L-\rho_G)}{\rho_L^2}\right]^{0.25}$

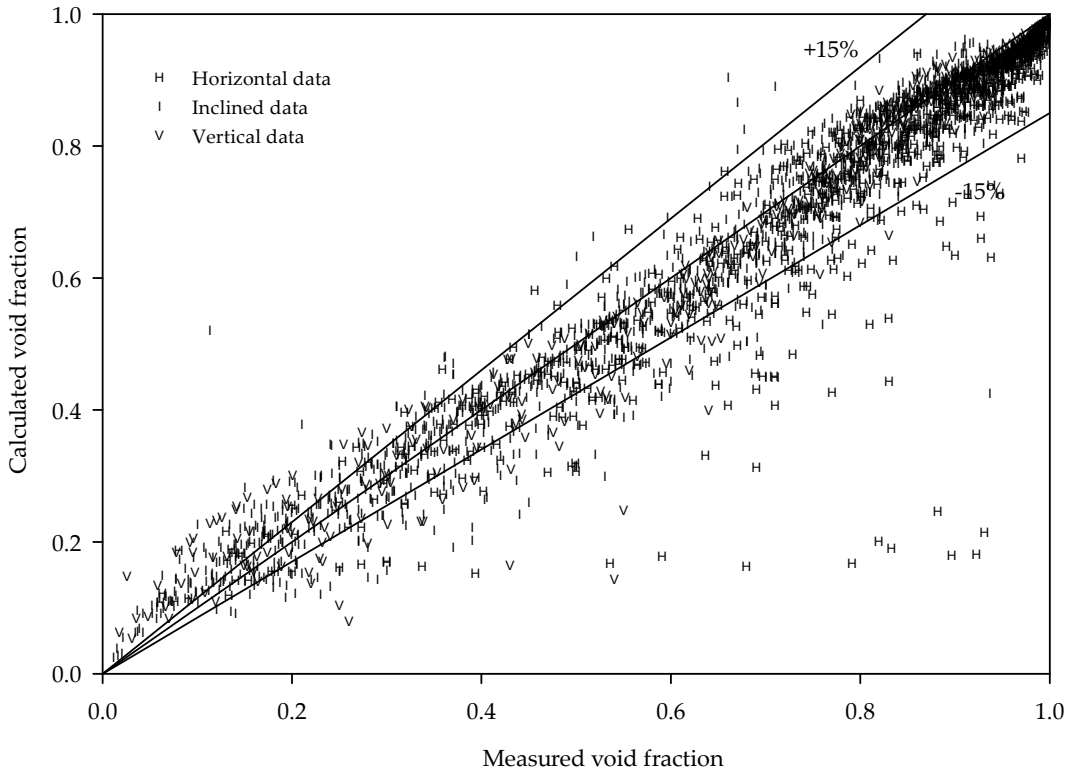

Fig. 1. Comparison of void fraction correlation by Dix [20] (see Table 3), with 2845 experimental data points summarized in Table 1, Woldesemayat and Ghajar [10].

The performance of Eq. (2) on the 2845 experimental data points in comparison with the recommended six void fraction correlations is also summarized in Table 2. As

shown in Table 2, the void fraction correlation, Eq. (2), introduced by Woldesemayat and Ghajar [10] gives noticeable improvements over the other six correlations. The results of the comparison for Eq. (2) with the 2845 experimental data points are also illustrated in Fig. 2. Both Table 2 and Fig. 2 show the capability and robustness of Eq. (2) to successfully predict void fraction for various pipe sizes, inclinations, and two-phase fluid mixtures from various sources with different experimental facilities. The benefit of comparing with experimental data from different facilities is the minimization of sample bias.

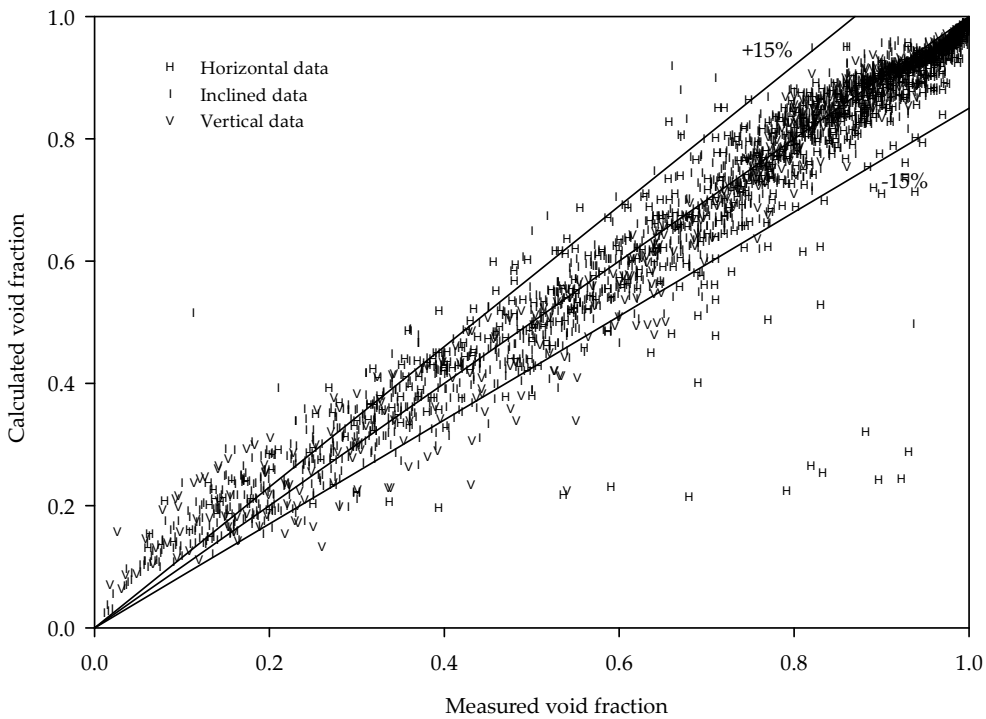

Fig. 2. Comparison of void fraction correlation by Woldesemayat and Ghajar [10], Eq. (2), with 2845 experimental data points summarized in Table 1, Woldesemayat and Ghajar [10].

Comparison of void fraction correlations for vertical pipes

Further scrutiny has also been done specifically on the performances of available void fraction correlations with available experimental data for upward vertical two-phase flow. The work demonstrated that more accurate predictions can be obtained by giving attention to specific pipe inclination and ranges of void fraction. The effort resulted in the categorization of void fraction correlations recommended for specific void fraction ranges in upward vertical two-phase flow. Results of these categorical comparisons would allow the access to correlations with higher accuracies for specific void fraction range of interest. A database with a total of 1208 experimental data points was used for the comparison with void fraction correlations available in the literature.

The database encompasses experimental data points for different gas-liquid combinations and pipe diameters. Table 4 presents a summary of the experimental database, compiled from ten independent sources, for the comparison with void fraction correlations.

In total, 52 flow pattern independent void fraction correlations are considered and compared with data points in the experimental database. Out of the 52 correlations, 11 correlations were considered to be in generally good agreement with the entire experimental database of 1208 data points. The 11 correlations were selected on the basis that their predictions, when compared with the experimental data, have more than 75% and 85% of the predicted data points within ±15% and ±20% error bands, respectively. The sources of the 11 selected correlations are listed in Table 5, along with the results of the comparison.

The 11 correlations listed in Table 5 were selected on the basis of overall performance, which overlooks the strengths and weaknesses in specific ranges of void fraction. Hence, the subsequent logical approach is to analyze the selected correlations in ranges, by dividing the entire void fraction range into four ranges: 0 to 0.25, 0.25 to 0.5, 0.5 to 0.75, and 0.75 to 1.0. The qualitative outcome of the 11 correlations and their performances in each of the four ranges are summarized in Table 6. By comparing the void fraction correlations with experimental data in each of the four specific ranges, the correlation by Rouhani & Axelsson [21] was identified as the best correlation for upward vertical two-phase flow. Figures 3 and 4 show the comparison of the Rouhani & Axelsson [21] and Nicklin *et al.* [26] correlations with the entire experimental database listed in Table 4. Although Table 5 indicates that the correlation by Nicklin *et al.* [26] has predicted more data points within the error bands of ±15% and ±20% than the correlation by Rouhani & Axelsson [21], it was noted that the Nicklin *et al.* [26] correlation performed unsatisfactorily in the 0.75 to 1.0 void fraction range. The Rouhani & Axelsson [21] correlation, on the other hand, is the only correlation that was found to perform satisfactorily on each of the four void faction ranges (see Table 6).

Table 4. Summary of experimental database for upward vertical two-phase flow.

Source	Pipe diameter [mm]	Fluids	No. of data points
Present study ‡	12.7	Air-water	153
Schmidt *et al.* [27]	54.5	Nitrogen-water	20
Sujumnong [18]	12.7	Air-water	104
Sujumnong [18]	12.7	Air-glycerin	77
Chokshi [28]	76.0	Air-water	103
Fernandes [29]	50.7	Air-water	88
Mukherjee [14]	38.1	Air-kerosene	65
Spedding & Nguyen [13]	45.5	Air-water	224
Beggs [12]	25.4 & 38.1	Air-water	27
Oshinowo [30]	25.4	Air-water	153
Oshinowo [30]	25.4	Air-glycerin	172
Isbin *et al.* [31]	22.2	Steam-water	22

‡ The experimental results of present study are discussed in a subsequent section.

Table 5. Results of the selected 11 correlations that compared satisfactorily with all 1208 experimental data points listed in Table 4.

Correlation	Percentage of data points predicted within the error band of			
	±5%	±10%	±15%	±20%
Nicklin *et al.* [26]	33.1	62.1	84.4	91.7
Hughmark [22]	33.9	58.2	76.7	86.1
Nishino & Yamazaki [32]	43.2	66.6	78.6	84.7
Guzhov *et al.* [33]	28.1	54.6	77.6	88.7
Rouhani & Axelsson [21]	39.9	68.5	83.5	89.3
Bonnecaze *et al.* [34]	33.1	62.1	84.4	91.7
Ishii [35]	37.9	66.6	80.5	87.3
Sun *et al.* [36]	31.3	58.1	78.1	91.1
Kokal & Stanislav [37]	33.0	61.9	84.4	91.6
Morooka *et al.* [19]	32.5	62.1	79.1	87.9
Takeuchi *et al.* [38]	27.6	52.7	78.1	88.6

Table 6. Qualitative performance of 11 selected correlations in four void fraction ranges.

Correlation	Void fraction range			
	0 to 0.25	0.25 to 0.50	0.50 to 0.75	0.75 to 1.0
Nicklin *et al.* [26]	S	S	S	NS
Hughmark [22]	NS	NS	S	S
Nishino & Yamazaki [32]	NS	NS	S	S
Guzhov *et al.* [33]	S	NS	S	S
Rouhani & Axelsson [21]	S	S	S	S
Bonnecaze *et al.* [34]	S	S	S	NS
Ishii [35]	S	NS	S	S
Sun *et al.* [36]	S	S	S	NS
Kokal & Stanislav [37]	S	S	S	NS
Morooka *et al.* [19]	S	NS	NS	S
Takeuchi *et al.* [38]	S	S	NS	NS

Note: S = satisfactory & NS = not satisfactory

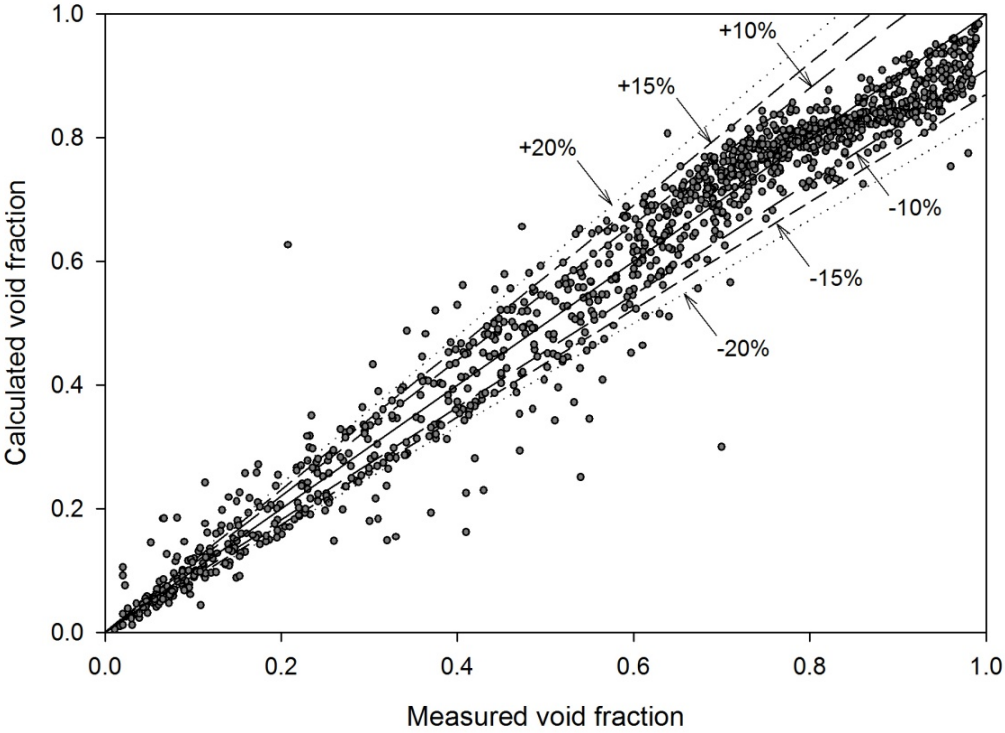

Fig. 3. Comparison of void fraction correlation by Rouhani & Axelsson [21], with 1208 experimental data points summarized in Table 4.

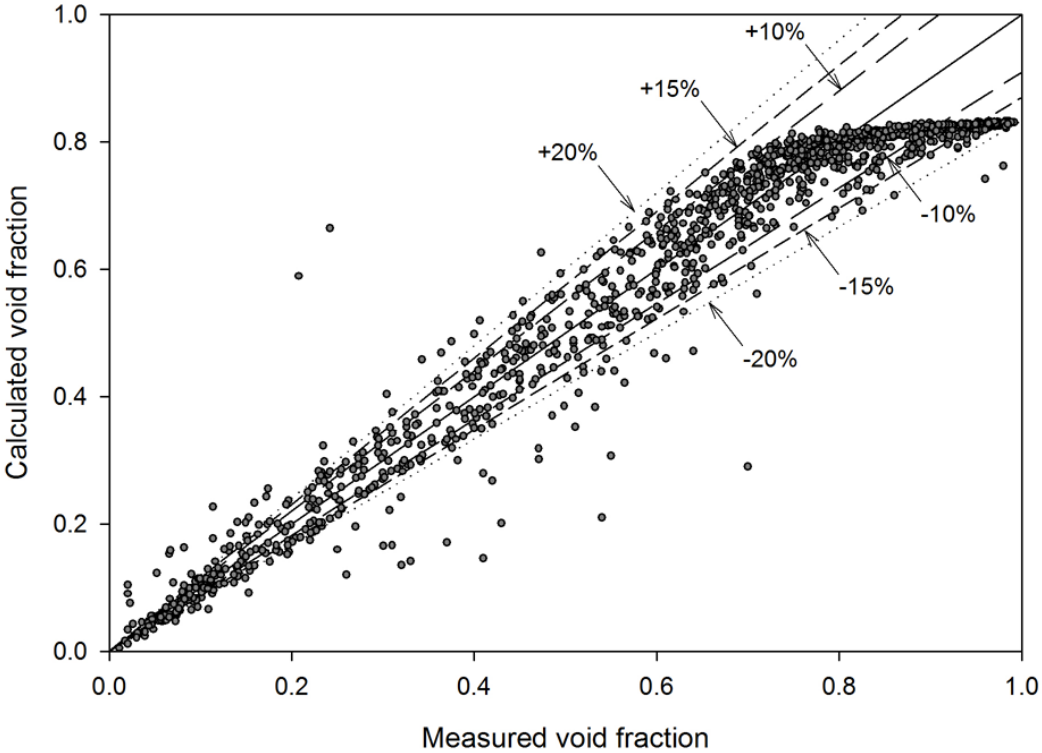

Fig. 4. Comparison of void fraction correlation by Nicklin *et al.* [26], with 1208 experimental data points summarized in Table 4.

Table 7. The experimental data used in Kim *et al.* [39].

Source	Orientation	Fluids	No. of data points
Vijay [40]	Vertical	Air-water	139
Vijay [40]	Vertical	Air-glycerin	57
Rezkallah [41]	Vertical	Air-silicone	162
Aggour [42]	Vertical	Helium-water	53
Aggour [42]	Vertical	Freon 12-water	44
Pletcher [43]	Horizontal	Air-water	48
King [44]	Horizontal	Air-water	21

Table 8. List of recommended correlations from the general comparisons with regard to fluid combinations and major flow patterns, Kim *et al.* [39].

Source	Heat transfer correlations
Aggour [42]	$h_{TP}/h_L = (1-\alpha)^{-1/3}$ Laminar where $\mathrm{Nu}_L = 1.615(\mathrm{Re}_{SL}\,\mathrm{Pr}_L\,D/L)^{1/3}(\mu_B/\mu_w)^{0.14}$ $h_{TP}/h_L = (1-\alpha)^{-0.83}$ Turbulent where $\mathrm{Nu}_L = 0.0155\mathrm{Re}_{SL}^{0.83}\,\mathrm{Pr}_L^{0.5}(\mu_B/\mu_w)^{0.33}$
Chu & Jones [45]	$\mathrm{Nu}_{TP} = 0.43\,\mathrm{Re}_{TP}^{0.55}\,\mathrm{Pr}_L^{1/3}\left(\frac{\mu_B}{\mu_w}\right)^{0.14}\left(\frac{P_{atm}}{P_{sys}}\right)^{0.17}$
Knott *et al.* [48]	$\frac{h_{TP}}{h_L} = \left(1+\frac{V_{SG}}{V_{SL}}\right)^{1/3}$ where h_L is from Sieder & Tate [49]
Kudirka *et al.* [50]	$\mathrm{Nu}_{TP} = 125\left(\frac{V_{SG}}{V_{SL}}\right)^{1/8}\left(\frac{\mu_G}{\mu_L}\right)^{0.6}\mathrm{Re}_{SL}^{1/4}\,\mathrm{Pr}_L^{1/3}\left(\frac{\mu_B}{\mu_w}\right)^{0.14}$
Martin & Sims [51]	$\frac{h_{TP}}{h_L} = 1+0.64\left(\frac{V_{SG}}{V_{SL}}\right)^{1/2}$ where h_L is from Sieder & Tate [49]
Ravipudi & Godbold [46]	$\mathrm{Nu}_{TP} = 0.56\left(\frac{V_{SG}}{V_{SL}}\right)^{0.3}\left(\frac{\mu_G}{\mu_L}\right)^{0.2}\mathrm{Re}_{SL}^{0.6}\,\mathrm{Pr}_L^{1/3}\left(\frac{\mu_B}{\mu_w}\right)^{0.14}$
Rezkallah & Sims [52]	$\frac{h_{TP}}{h_L} = (1-\alpha)^{-0.9}$ where h_L is from Sieder & Tate [49]
Shah [53]	$\frac{h_{TP}}{h_L} = \left(1+\frac{V_{SG}}{V_{SL}}\right)^{1/4}$ where $\mathrm{Nu}_L = 1.86(\mathrm{Re}_{SL}\,\mathrm{Pr}_L\,D/L)^{1/3}(\mu_B/\mu_w)^{0.14}$ Laminar $\mathrm{Nu}_L = 0.023\mathrm{Re}_{SL}^{0.8}\,\mathrm{Pr}_L^{0.4}(\mu_B/\mu_w)^{0.14}$ Turbulent

Note: α is taken from the original experimental data. $\mathrm{Re}_{SL} < 2000$ implies laminar flow, otherwise turbulent; and for Shah [53], replace 2000 by 170. With regard to the eqs. given for Shah [53] above, the laminar two-phase correlation was used along with the appropriate single phase correlation, since Shah [53] recommended a graphical turbulent two-phase correlation.

Table 9. Results of recommended correlations with regard to fluid combinations and major flow patterns, Kim *et al.* [39].

Correlations	Vertical pipes												
	Air-water				Air-glycerin				Air-silicone				
	B	S	F	A	B	S	F	A	B	S	C	A	F
Aggour [42]	√	√			√	√	√	√					
Chu & Jones [45]				√									
Knott *et al.* [48]			√										√
Kudirka *et al.* [50]													
Martin & Sims [51]	√												
Ravipudi & Godbold [46]				√							√	√	
Rezkallah & Sims [52]	√								√	√	√		
Shah [53]	√		√		√				√				√

Correlations	Vertical pipes								Horizontal pipes	
	Helium-water				Freon 12-water				Air-water	
	B	S	F	A	B	S	F	A	A	S
Aggour [42]					√	√	√	√		
Chu & Jones [45]	√		√				√			√
Knott *et al.* [48]	√	√	√		√		√			
Kudirka *et al.* [50]										√
Martin & Sims [51]	√				√	√	√	√		√
Ravipudi & Godbold [46]						√				√
Rezkallah & Sims [52]	√				√	√	√	√		
Shah [53]	√		√		√		√		√	

Note: √ = Recommended correlation with and without restrictions. Shaded cells indicate the correlations that best satisfied the ±30% two-phase heat transfer coefficient criterion.
A = annular, B = bubbly, C = churn, F = froth, S = slug.

Comparison of Twenty Two-Phase Heat Transfer Correlations with Seven Sets of Experimental Data

Numerous heat transfer correlations and experimental data for forced convective heat transfer during gas-liquid two-phase flow in vertical and horizontal pipes have been published over roughly the past six decades. In a study published by Kim *et al.* [39], a comprehensive literature search was carried out and a total of 38 two-phase flow heat transfer correlations were identified. The validity of these correlations and their ranges of applicability have been documented by the original authors. In most cases, the identified heat transfer correlations were based on a small set of experimental data with a limited range of variables and gas-liquid combinations. In order to assess the validity of those correlations, they were compared against seven extensive sets of two-phase flow heat transfer experimental data available from the literature, for vertical and horizontal tubes and different flow patterns and fluid combinations. For consistency, the validity of the identified heat transfer correlations were based on the comparison between the predicted and experimental two-phase heat transfer coefficients meeting the ±30% criterion. Out of the 38 two-phase flow heat transfer correlations, Kim *et al.* [39] identified 20 correlations for comparison with experimental data from the various sources. Eighteen of the 38 two-phase flow heat transfer correlations were not tested,

since the required information for those correlations was not available through the identified experimental studies.

A total of 524 data points from the five available experimental studies [40-44] were used for these comparisons (see Table 7). The experimental data included five different gas-liquid combinations (air-water, air-glycerin, air-silicone, helium-water, Freon 12-water), and covered a wide range of variables, including liquid and gas flow rates and properties, flow patterns, pipe sizes, and pipe inclination. Five of these experimental data sets are concerned with a wide variety of flow patterns in vertical pipes and the other two data sets are for limited flow patterns (slug and annular) within horizontal pipes. In assessing the ability of the 20 identified heat transfer correlations, their predictions were compared with the experimental data from the sources listed in Table 7, both with and without considering the restrictions on superficial liquid Reynolds number (Re_{SL}) and superficial gas velocity to superficial liquid velocity ratio (V_{SG}/V_{SL}) accompanying the correlations. The two-phase flow heat transfer correlations recommended by Kim *et al.* [39] from the general comparisons with regard to fluid combinations and major flow patterns are listed in Table 8. The results from comparing the 20 two-phase flow heat transfer correlations and the experimental data are several correlations for major flow patterns recommended by Kim *et al.* [39], which are summarized in Table 9.

There were no remarkable differences for the recommendations of the heat transfer correlations based on the results with and without the restrictions on Re_{SL} and V_{SG}/V_{SL}, except for the correlations of Chu and Jones [45] and Ravipudi and Godbold [46], as applied to the air-water experimental data of Vijay [40]. Details of this discussion can be found in Kim *et al.* [39]. Based on the results without the authors' restrictions on Re_{SL} and V_{SG}/V_{SL}, the correlation of Chu and Jones [45] was recommended for only annular, bubbly-froth, slug-annular, and froth-annular flow patterns of air-water in vertical pipes. While the correlation of Ravipudi and Godbold [46] was recommended for only annular, slug-annular, and froth-annular flow patterns of air-water in vertical pipes. However, when considering the Re_{SL} and V_{SG}/V_{SL} restrictions by the authors, the correlation of Chu and Jones [45] was recommended for all vertical pipe air-water flow patterns including transitional flow patterns except the annular-mist flow pattern. While the correlation of Ravipudi and Godbold [46] was recommended for slug, froth, and annular flow patterns and for all of the transitional flow patterns of the vertical air-water experimental data.

All of the above recommended correlations have the following important parameters in common: Re_{SL}, Pr_L, μ_B/μ_w and either void fraction (α) or superficial velocity ratio (V_{SG}/V_{SL}). It appears that void fraction and superficial velocity ratio, although not directly related, may serve the same function in two-phase flow heat transfer correlations. From the comprehensive literature search, Kim *et al.* [39] found that there is no single correlation capable of predicting the flow for all fluid combinations in vertical pipes. In the following section, the effort of Kim *et al.* [47] in developing a heat transfer correlation that is robust enough to span all or most of the fluid combinations and flow patterns for vertical pipes is highlighted. Kim *et al.* [47] developed a correlation that is capable of predicting heat transfer coefficient in two-phase flow regardless of fluid combinations and flow patterns. The correlation uses a carefully

derived heat transfer model which takes into account the appropriate contributions of both the liquid and gas phases using the respective cross-sectional areas occupied by the two phases.

Development of a Heat Transfer Correlation for Vertical Pipes

In this section, the effort of Kim *et al.* [47] in developing a heat transfer correlation that is robust enough to span all or most of the fluid combinations and flow patterns for vertical pipes is highlighted. The void fraction (α) is defined as the ratio of the gas-flow cross-sectional area (A_G) to the total cross-sectional area, A (= $A_G + A_L$),

$$\alpha = \frac{A_G}{A_G + A_L} \tag{3}$$

The actual gas velocity (V_G) can be calculated from

$$V_G = \frac{Q_G}{A_G} = \frac{\dot{m}_G}{\rho_G A_G} = \frac{\dot{m}x}{\rho_G \alpha A} \tag{4}$$

Similarly, the actual liquid velocity (V_L) is defined as

$$V_L = \frac{Q_L}{A_L} = \frac{\dot{m}_L}{\rho_L A_L} = \frac{\dot{m}(1-x)}{\rho_L (1-\alpha) A} \tag{5}$$

The total gas-liquid two-phase heat transfer coefficient is assumed to be the sum of the individual single-phase heat transfer coefficients of the gas and liquid phases, weighted by the volume of each phase

$$h_{TP} = (1-\alpha)h_L + \alpha h_G = (1-\alpha)h_L\left[1+\left(\frac{\alpha}{1-\alpha}\right)\left(\frac{h_G}{h_L}\right)\right] \tag{6}$$

Based upon this correlation, the single-phase heat transfer coefficients in Eq. (6), h_L and h_G, can be modeled as functions of Reynolds number, Prandtl number and the ratio of bulk to wall viscosities. Thus, Eq. (6) can be expressed as

$$h_{TP} = (1-\alpha)h_L\left[1+\frac{\alpha}{1-\alpha}\frac{f(\mathrm{Re},\mathrm{Pr},\mu_B/\mu_w)_G}{f(\mathrm{Re},\mathrm{Pr},\mu_B/\mu_w)_L}\right] \tag{7}$$

or

$$h_{TP} = (1-\alpha)h_L \left\{ 1 + \frac{\alpha}{1-\alpha} f\left[\frac{\mathrm{Re}_G}{\mathrm{Re}_L}, \frac{\mathrm{Pr}_G}{\mathrm{Pr}_L}, \frac{(\mu_B/\mu_w)_G}{(\mu_B/\mu_w)_L} \right] \right\} \tag{8}$$

Substituting the definition of Reynolds number (Re = $\rho VD/\mu_B$) for the gas (Re_G) and liquid (Re_L) yields

$$\frac{h_{TP}}{(1-\alpha)h_L} = 1 + \frac{\alpha}{1-\alpha} f\left[\frac{(\rho VD/\mu_B)_G}{(\rho VD/\mu_B)_L}, \frac{\mathrm{Pr}_G}{\mathrm{Pr}_L}, \frac{(\mu_B/\mu_w)_G}{(\mu_B/\mu_w)_L} \right] \tag{9}$$

Rearranging yields

$$\frac{h_{TP}}{(1-\alpha)h_L} = 1 + \frac{\alpha}{1-\alpha} f\left[\frac{\rho_G V_G D_G}{\rho_L V_L D_L}, \frac{\mathrm{Pr}_G}{\mathrm{Pr}_L}, \frac{(\mu_w)_L}{(\mu_w)_G} \right] \tag{10}$$

where the assumption has been made that the viscosity ratio in the Reynolds number term of Eq. (9) is exactly cancelled by the last term in Eq. (9), which includes the same viscosity ratio. Substituting Eq. (3) for the ratio of gas-to-liquid diameters (D_G/D_L) in Eq. (10) and based upon practical considerations assuming that the ratio of liquid-to-gas viscosities evaluated at the wall temperature is comparable to the ratio of those viscosities evaluated at the bulk temperature $(\mu_L/\mu_G)_B$, Eq. (10) reduces to

$$\frac{h_{TP}}{(1-\alpha)h_L} = 1 + \frac{\alpha}{1-\alpha} f\left(\frac{\rho_G V_G \sqrt{\alpha}}{\rho_L V_L \sqrt{1-\alpha}}, \frac{\mathrm{Pr}_G}{\mathrm{Pr}_L}, \frac{\mu_L}{\mu_G} \right) \tag{11}$$

Further simplifying Eq. (11), combine Eqs. (4) and (5) for gas velocity (V_G) and liquid velocity (V_L) to get the ratio of V_G/V_L and substitute into Eq. (11) to get

$$h_{TP} = (1-\alpha)h_L \left[1 + f\left(\frac{x}{1-x}, \frac{\alpha}{1-\alpha}, \frac{\mathrm{Pr}_G}{\mathrm{Pr}_L}, \frac{\mu_L}{\mu_G} \right) \right] \tag{12}$$

Assuming that two-phase heat transfer coefficient can be expressed using a power-law relationship on the individual parameters that appear in Eq. (12), then it can be expressed as

$$h_{TP} = (1-\alpha)h_L \left\{ 1 + C\left[\left(\frac{x}{1-x}\right)^m \left(\frac{\alpha}{1-\alpha}\right)^n \left(\frac{\mathrm{Pr}_G}{\mathrm{Pr}_L}\right)^p \left(\frac{\mu_G}{\mu_L}\right)^q \right] \right\} \tag{13}$$

where C, m , n, p, and q are adjustable constants, and h_L comes from the Sieder and Tate [49] correlation for turbulent flow,

$$h_L = 0.027\,\mathrm{Re}_L^{4/5}\,\mathrm{Pr}_L^{1/3}\left(\frac{k_L}{D}\right)\left(\frac{\mu_B}{\mu_W}\right)_L^{0.14} \tag{14}$$

Although there are several well-known single-phase heat transfer correlations in the literature. In this study the Sieder and Tate [49] equation was chosen as the fundamental single-phase heat transfer correlation because of its practical simplicity and proven applicability. Any other well-known single-phase turbulent heat transfer correlation could have been used in place of the Sieder and Tate [49] correlation. The difference resulting from the use of a different single-phase heat transfer correlation will be absorbed during the determination of the values of the leading coefficient and exponents on the different parameters in Eq. (13). For the Reynolds number (Re_L) in Eq. (14), the following relationship is used to evaluate the *in situ* Reynolds number (liquid phase) rather than the superficial Reynolds number (Re_{SL}) as commonly used in the correlations available in the literature [39]:

$$\mathrm{Re}_L = \left(\frac{\rho V D}{\mu}\right)_L = \frac{4\dot{m}_L}{\pi\sqrt{1-\alpha}\,\mu_L D} \tag{15}$$

The values of the void fraction (α) used in Eq. (13) were either taken directly from the original experimental data sets (if available) or were calculated based on the equation provided by Chisholm [54], which can be expressed as

$$\alpha = \left[1 + \left(1 - x + x\frac{\rho_L}{\rho_G}\right)^{1/2}\left(\frac{1-x}{x}\right)\left(\frac{\rho_G}{\rho_L}\right)\right]^{-1} \tag{16}$$

In the next section the proposed heat transfer correlation, Eq. (13), will be tested with four extensive sets of vertical two-phase flow heat transfer data available from the literature (see Table 7).

Heat Transfer Correlation for Gas-Liquid Flow in Vertical Pipes

Four sets of experimental data (see the first column in Table 10) for vertical pipe flow were used to validate the two-phase flow heat transfer correlation, Eq. (13), developed in previous section. The ranges of these four sets of experimental data can be found in Kim *et al.* [39]. The experimental data (a total of 255 data points) included four different gas-liquid combinations (air-water, air-silicone, helium-water, Freon 12-water), and covered a wide range of variables, including liquid and gas flow rates, properties, and flow patterns. The selected experimental data were only for turbulent two-phase heat transfer data in which the superficial Reynolds numbers of the liquid (Re_{SL}) were all greater than 4000. Table 10 and Fig. 5 provide the details of the correlation and how well the proposed correlation predicted the experimental data.The

two-phase heat transfer correlation, Eq. (13), predicted the heat transfer coefficients of 255 experimental data points for vertical flow with an overall mean deviation of about 2.5% and a root-mean-square deviation of about 12.8%. About 83% of the data (212 data points) were predicted with less than ±15% deviation, and about 96% of the data (245 data points) were predicted with less than ±30% deviation. The results clearly show that the proposed heat transfer correlation is robust and can be applied to turbulent gas-liquid flow in vertical pipes with different flow patterns and fluid combinations.

Table 10. Results of the predictions for available two-phase heat transfer experimental data in vertical pipes using Eq. (13), Kim *et al.* [47].

Fluids (Re_{SL} > 4000)	Values of constant and exponents					RMS dev. (%)	Mean dev. (%)	No. of data within ±30%	Range of parameters			
	C	m	n	p	q				Re_{SL}	Re_{SG}	Pr_G / Pr_L	μ_G / μ_L
All 255 data points	0.27	−0.04	1.21	0.66	−0.72	12.78	2.54	245	4000 to 127000	14 to 209000	9.99×10^{-3} to 137×10^{-3}	3.64×10^{-3} to 23.7×10^{-3}
Air-water [40] 105 data points						12.98	3.53	98				
Air-silicone [41] 56 data points						7.77	5.25	56				
Helium-water [42] 50 data points						15.68	−1.66	48				
Freon 12-water [42] 44 data points						13.74	1.51	43				

Only data points for Re_{SL} > 4000 are considered. Data of Vijay [40], see Table 7, for air-glycerin did not satisfy the Re_{SL} > 4000 condition.

A General Two-Phase Heat Transfer Correlation for Various Flow Patterns and Pipe Inclinations

The heat transfer correlation developed by Kim *et al.* [47], Eq. (13), was meant for predicting heat transfer rate in two-phase flow in vertical pipes. In order to handle the effects of various flow patterns and inclination angles on the two-phase heat transfer data with only one correlation, Ghajar and Kim [55] and Kim and Ghajar [56] introduced the flow pattern factor (F_P) and the inclination factor (I). The void fraction (α), which is the volume fraction of the gas-phase in the tube cross-sectional area, does not reflect the actual wetted-perimeter (S_L) in the tube with respect to the corresponding flow pattern. For instance, the void fraction and the non-dimensionalized wetted-perimeter of annular flow both approach unity, but in the case of plug flow the void fraction is near zero and the wetted-perimeter is near unity. However, the estimation of the actual wetted-perimeter is very difficult due to the continuous interaction of the two phases in the tube. Therefore, instead of estimating the actual wetted-perimeter, modeling the effective wetted-perimeter is a more practical approach. In their model, Ghajar and his co-workers have ignored the influence of the surface tension and the

contact angle of each phase on the effective wetted-perimeter. The wetted-perimeter at the equilibrium state, which can be calculated from the void fraction, is

$$\widetilde{S}_{L,eq}^{2} = \left(\frac{S_{L,eq}}{\pi D} \right)^{2} = 1 - \alpha \tag{17}$$

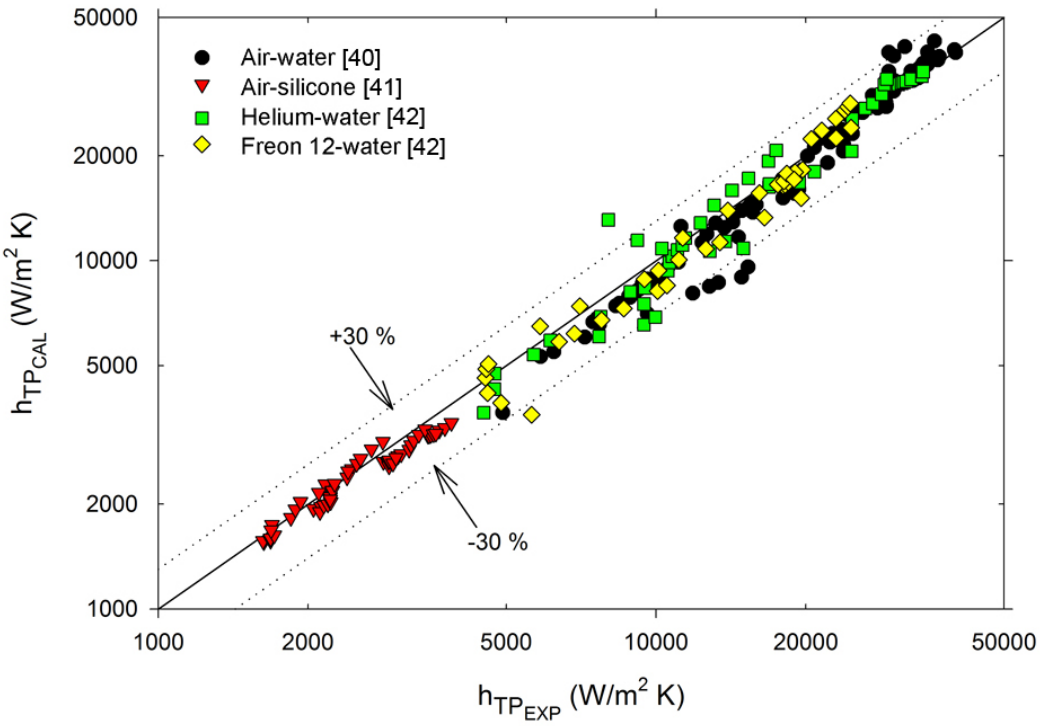

Fig. 5. Comparison of the predictions by Eq. (13) with the experimental data for vertical flow (255 data points), Kim *et al.* [47].

However, as shown in Fig. 6, the shape of the gas-liquid interface at the equilibrium state based on the void fraction (α) is far different from the one for the realistic case. The two-phase heat transfer correlation, Eq. (13), weighted by the void fraction ($1-\alpha$), is not capable of distinguishing the differences between different flow patterns. Therefore, in order to capture the realistic shape of the gas-liquid interface, the flow pattern factor (F_P), an effective wetted-perimeter relation, which is a modified version of the equilibrium wetted-perimeter, Eq. (17), is proposed,

$$F_P = \widetilde{S}_{L,eff}^{2} = \left(\frac{S_{L,eff}}{\pi D} \right)^{2} = (1-\alpha) + \alpha F_S^2 \tag{18}$$

For simplicity, the equation for the effective wetted-perimeter relation, Eq. (18), is referred to as the flow pattern factor (F_P). The term (F_S) appearing in Eq. (18) is referred to as shape factor which in essence is a modified and normalized Froude number. The shape factor (F_S) is defined as

$$F_S = \frac{2}{\pi}\tan^{-1}\left(\sqrt{\frac{\rho_G\left(V_G - V_L\right)^2}{g\,D\left(\rho_L - \rho_G\right)}}\right) \tag{19}$$

The shape factor (F_S) is applicable for slip ratio greater than or equal to one ($K \geq 1$), which is common in gas-liquid flow, and represents the shape changes of the gas-liquid interface by the force acting on the interface due to the relative momentum and gravitational forces.

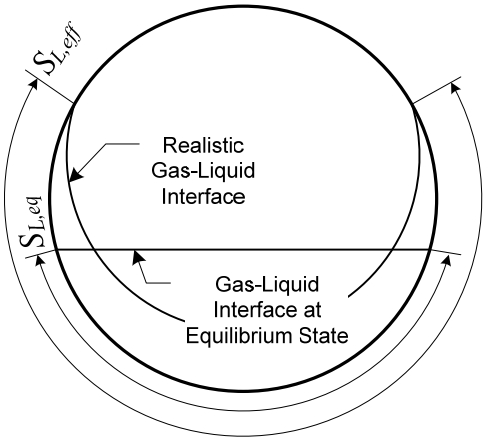

Fig. 6. Gas-liquid interfaces and wetted-perimeters.

Due to the density difference between gas and liquid, the liquid phase is much more affected by the orientation of pipe (inclination). The detailed discussion of the inclination effect on the two-phase heat transfer is available in Ghajar and Tang [57]. In order to account for the effect of inclination, Ghajar and Kim [55] proposed the inclination factor

$$I = 1 + \frac{g\,D\left(\rho_L - \rho_G\right)\sin\theta}{\rho_L V_{SL}^2} \tag{20}$$

The expression for the inclination factor (I), Eq. (20), includes representation of the relative force acting on the liquid phase in the flow direction due to the momentum and the buoyancy forces.

The two proposed factors for the flow pattern (F_P) and pipe inclination (I) effects are introduced into the two-phase heat transfer correlation for vertical pipe, Eq. (13). By substituting (F_P) for ($1-\alpha$) which is the leading coefficient of (h_L) and introducing (I) as

an additional power-law term in Eq. (13), the two-phase heat transfer correlation becomes

$$h_{TP} = F_P h_L \left\{ 1 + C \left[\left(\frac{x}{1-x} \right)^m \left(\frac{1-F_P}{F_P} \right)^n \left(\frac{Pr_G}{Pr_L} \right)^p \left(\frac{\mu_L}{\mu_G} \right)^q (I)^r \right] \right\} \tag{21}$$

where (h_L) comes from the Sieder and Tate [49] correlation for turbulent flow, see Eq. (14). For the Reynolds number needed in the (h_L) calculation, Eq. (15) presented and discussed earlier was used. The values of the void fraction (α) used in Equations (15), (18), and (21) were calculated based on the correlation provided by Woldesemayat and Ghajar [10], which was given by Eq. (2).

Other void fraction correlations could also be used in place of the Woldesemayat and Ghajar [10] correlation. Tang and Ghajar [58] showed that Eq. (21) has the robustness that it can be applied with different void fraction correlations. The difference resulting from the use of different correlations will be absorbed during the determination of the values of the constant and exponents of Eq. (21). The two-phase heat transfer correlation, Eq. (21) was validated with a total of 763 experimental data points for different flow patterns and inclination angles [56, 58, 59]. Overall, the correlation, Eq. (21), has successfully predicted over 85% of the experimental data points to within ±30% for 0°, 2°, 5°, and 7° pipe orientations.

However, upon revisiting the two-phase heat transfer correlation, Eq. (21), along with the equations for flow pattern factor (F_P), Eq. (18), and inclination factor (I), Eq. (20), it was realized that the correlation has not accounted for the surface tension force. Since surface tension is a variable that can affect the hydrodynamics of gas-liquid two-phase flow, it is sensible to include the surface tension into the correlation. In order to do that, the equation for the inclination factor (I), Eq. (20), is modified. The modified inclination factor takes on the following form,

$$I^* = 1 + \mathrm{Eo} \left| \sin\theta \right| \tag{22}$$

where the Eötvös number (Eo) is defined as

$$\mathrm{Eo} = \frac{(\rho_L - \rho_G) g D^2}{\sigma} \tag{23}$$

The Eötvös number (Eo), also known as Bond number (Bo), represents the hydrodynamic interaction of buoyancy and surface tension forces that occur in two-phase flow. With the modification of the equation for the inclination factor, two-phase heat transfer coefficients can be estimated using the general two-phase heat transfer correlation, Eq. (21), along with the flow pattern factor (F_P), Eq. (18), and modified inclination factor (I^*), Eq. (23),

$$h_{TP} = F_P\, h_L \left[1 + C\left(\frac{x}{1-x}\right)^m \left(\frac{1-F_P}{F_P}\right)^n \left(\frac{Pr_G}{Pr_L}\right)^p \left(\frac{\mu_L}{\mu_G}\right)^q (I^*)^r \right] \tag{24}$$

The proper values of the constant and exponents are discussed in a later section.

Experimental Setup

Experimental setup for horizontal and slightly upward inclined flow

A schematic diagram of the overall experimental setup for heat transfer measurements is shown in Fig. 7. The test section is a straight standard stainless steel schedule 10S pipe with an inner diameter of 27.9 mm and a length to diameter ratio of 95. The setup rests atop a 9-m long aluminum I-beam that is supported by a pivoting foot and a stationary foot that incorporates a small electric screw jack. In order to apply uniform wall heat flux boundary condition to the test section, copper plates were silver soldered to the inlet and exit of the test section. The uniform wall heat flux boundary condition was maintained by a Lincoln SA-750 welder for superficial liquid Reynolds number greater than 2000 and a Miller Maxtron 450 DC welder for superficial liquid Reynolds number less than 2000. The Lincoln SA-750 welder has the capability of supplying 300 to 750 A of current, while the Miller Maxtron 450 DC welder is capable of supplying 5 to 450 A of current. The entire length of the test section was wrapped using fiberglass pipe wrap insulation, followed by a thin polymer vapor seal to prevent moisture penetration. The calming section (clear polycarbonate pipe with inner diameter of 25.4 mm and length to diameter ratio of 88) served as a flow developing and turbulence reduction device, and flow pattern observation section. One end of the calming section is connected to the test section with an acrylic flange and the other end of the calming section is connected to the gas-liquid mixer. For the horizontal flow measurements, the test section, and the observation section (refer to Fig. 7) were carefully leveled to eliminate the effect of inclination on these measurements.

T-type thermocouple wires were cemented with Omegabond 101, an epoxy adhesive with high thermal conductivity and electrical resistivity, to the outside wall of the stainless steel test section as shown in Fig. 8. Thermocouples were placed on the outer surface of the pipe wall at uniform intervals of 254 mm from the entrance to the exit of the test section. There were 10 thermocouple stations in the test section (refer to Fig. 8). All the thermocouples were monitored with a National Instruments data acquisition system. The average system stabilization time period was from 30 to 60 minutes after the system attained steady state. The inlet liquid and gas temperatures and the exit bulk temperature were measured by Omega TMQSS-125U-6 thermocouple probes. Calibration of thermocouples and thermocouple probes showed that they were accurate within ±0.5°C. The operating pressures inside the experimental setup were monitored with a pressure transducer. To ensure a uniform fluid bulk temperature at the inlet and exit of the test section, a mixing well of alternating polypropylene baffle type static mixer for both gas and liquid phases was utilized.

The fluids used in the test loop are air and water. The water is distilled and stored in a 55-gallon cylindrical polyethylene tank. A Bell & Gosset series 1535 coupled centrifugal pump was used to pump the water through an Aqua-Pure AP12T water filter. An ITT Standard model BCF 4063 one shell and two-tube pass heat exchanger removes the pump heat and the heat added during the test to maintain a constant inlet water temperature. From the heat exchanger, the water passes through a Micro Motion Coriolis flow meter (model CMF100) connected to a digital Field-Mount Transmitter (model RFT9739) that conditions the flow information for the data acquisition system. From the Coriolis flow meter it then flows into the test section. Air is supplied via an Ingersoll-Rand T30 (model 2545) industrial air compressor. The air passes through a copper coil submerged in a vessel of water to lower the temperature of the air to room temperature. The air is then filtered and condensation removed in a coalescing filter. The air flow is measured by a Micro Motion Coriolis flow meter (model CMF025) connected to a digital Field-Mount Transmitter (model RFT9739) and regulated by a needle valve. Air is delivered to the test section by flexible tubing. The water and air mixture is returned to the reservoir where it is separated and the water recycled.

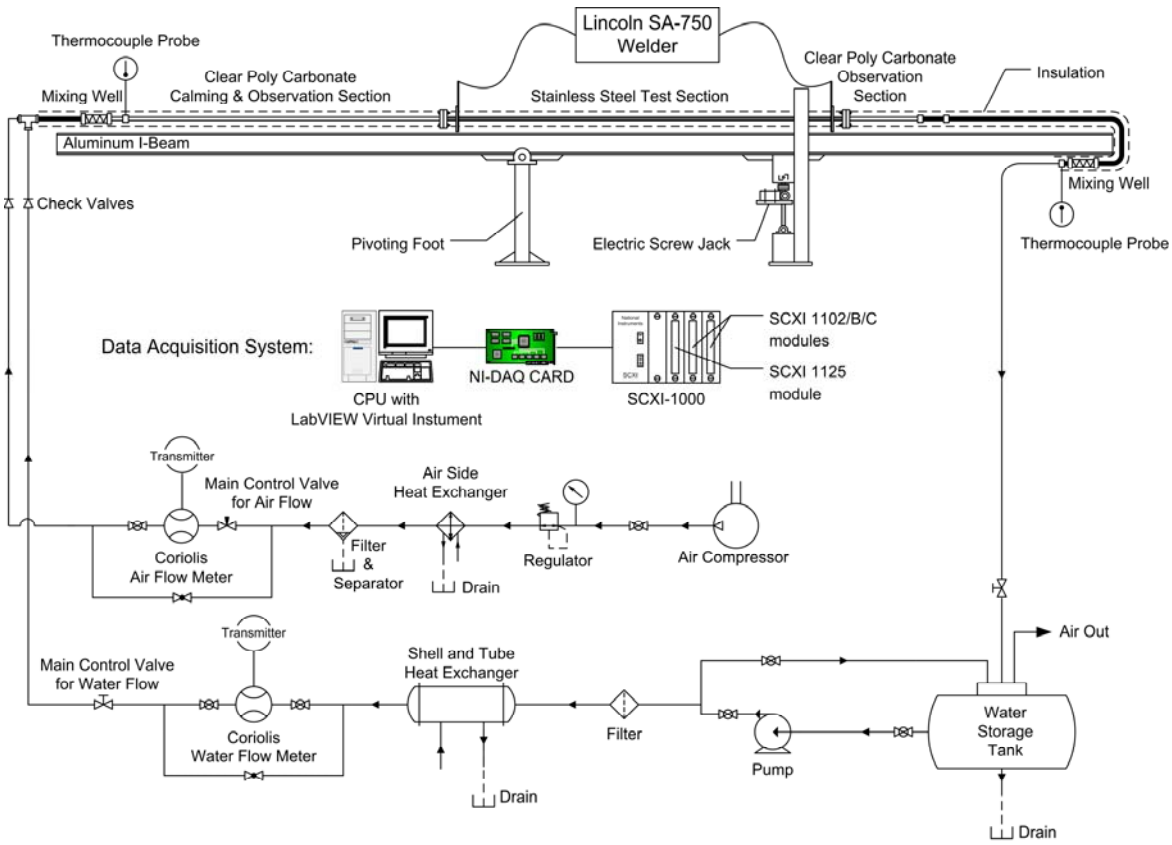

Fig. 7. Schematic of experimental setup.

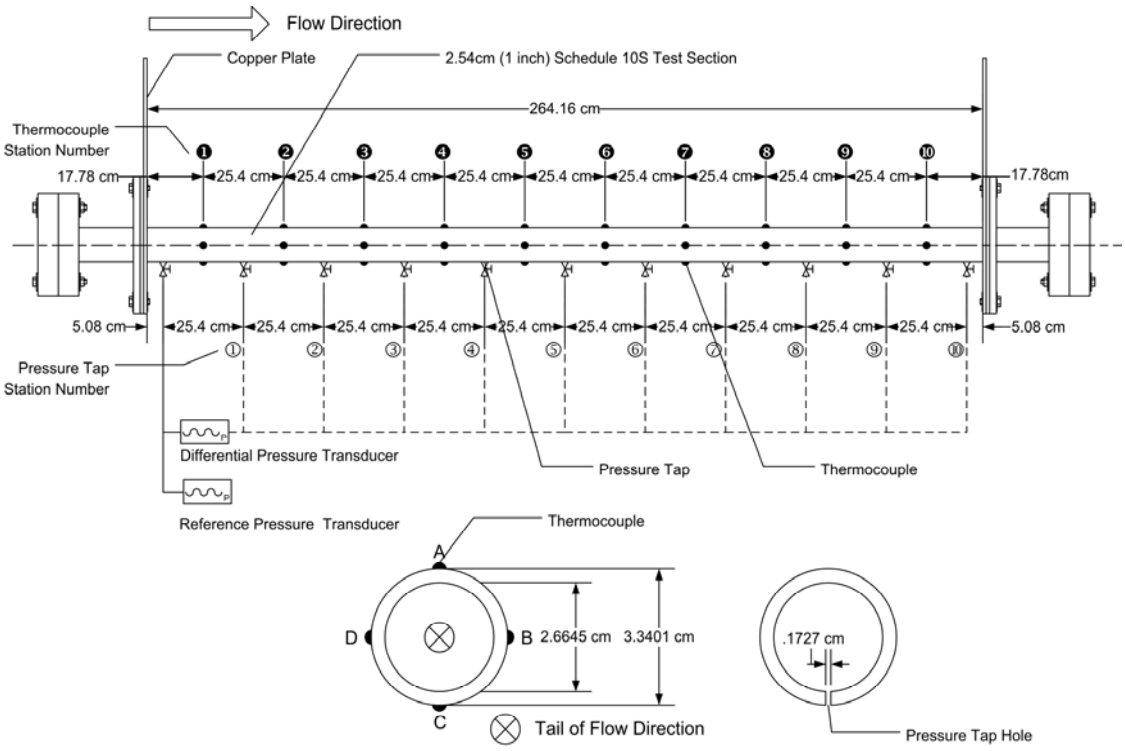

Fig. 8. Schematic of heated test section illustrating the placement of thermocouples.

The heat transfer measurements at uniform wall heat flux boundary condition were carried out by measuring the local outside wall temperatures at 10 stations along the axis of the pipe and the inlet and outlet bulk temperatures in addition to other measurements such as the flow rates of gas and liquid, room temperature, voltage drop across the test section, and current carried by the test section. A National Instruments data acquisition system was used to record and store the data measured during these experiments. The computer interface used to record the data is a LabVIEW Virtual Instrument (VI) program written for this specific application. The peripheral heat transfer coefficient (local average) was calculated based on the knowledge of the pipe inside wall surface temperature and inside wall heat flux obtained from a data reduction program developed exclusively for this type of experiments [60]. The local average peripheral values for inside wall temperature, inside wall heat flux, and heat transfer coefficient were then obtained by averaging all the appropriate individual local peripheral values at each axial location. The variation in the circumferential wall temperature distribution, which is typical for two-phase gas-liquid flow in horizontal pipes, leads to different heat transfer coefficients depending on which circumferential wall temperature was selected for the calculations. In two-phase heat transfer experiments, in order to overcome the unbalanced circumferential heat transfer coefficients and to get a representative heat transfer coefficient for a test run, the following equation was used to calculate an overall two-phase heat transfer coefficient ($h_{TP_{EXP}}$) for each test run:

$$h_{TP_{EXP}} = \frac{1}{L}\int \bar{h}\, dz = \frac{1}{L}\sum_{k=1}^{N_{ST}} \bar{h}_k\, \Delta z_k = \frac{1}{L}\sum_{k=1}^{N_{ST}} \left(\frac{\overline{\dot{q}''}}{\overline{T}_w - T_B} \right)_k \Delta z_k \tag{25}$$

where L is the length of the test section, $\bar{h}$, $\overline{\dot{q}''}$, $\overline{T}_w$, T_B are the local mean heat transfer coefficient, the local mean heat flux, the local mean wall temperature, and the bulk temperature at a thermocouple station, respectively; k is the index of the thermocouple stations, N_{ST} is the number of the thermocouple stations, z is the axial coordinate, and Δz is the element length of each thermocouple station. The data reduction program used a finite-difference formulation to determine the inside wall temperature and the inside wall heat flux from measurements of the outside wall temperature, the heat generation within the pipe wall, and the thermophysical properties of the pipe material (electrical resistivity and thermal conductivity).

The reliability of the flow circulation system and of the experimental procedures was checked by making several single-phase calibration runs with distilled water. The single-phase heat transfer experimental data were checked against the well established single-phase heat transfer correlations [61] in the Reynolds number range from 3000 to 30,000. In most instances, the majority of the experimental results were well within ±10% of the predicted results [61, 62]. The uncertainty analysis of the overall experimental procedures using the method of Kline and McClintock [63] showed that there is a maximum of 11.5% uncertainty for heat transfer coefficient calculations. Experiments under the same conditions were conducted periodically to ensure the repeatability of the results. The maximum difference between the duplicated experimental runs was within ±10%.

Experimental setup for horizontal to upward and downward vertical flow

The recently constructed experimental setup is equipped for measuring heat transfer, pressure drop, void fraction, and also conducting flow visualization in air-water flow for all major flow patterns and inclination angles from 0° (horizontal) to ±90° (vertical). The capabilities of the new experimental setup allow an undertaking that combines the study of heat transfer, flow patterns, pressure drop, void fraction, and inclination effects. The flow loop using air and water for this experimental setup is similar to that illustrated in Fig. 7. Detail discussions on the design, construction and functionality of this experimental setup are documented by Cook [64].

In this writing, only the experimental results of flow patterns and void fraction in upward vertical flow are discussed. The test section for flow visualization and void fraction is illustrated in Fig. 9. The flow visualization section is the central portion of the void fraction section. The flow visualization section is constructed from a polycarbonate tube with an inner diameter of 12.7 mm. Pressure taps are included in the flow visualization section for measuring pressure drop across the section.

The void fraction section is constructed to trap mixture of two-phase flow in order to measure the volume of the liquid portion. With the known volume of the void fraction section and the measured volume of the liquid portion, the value of the void fraction can be determined. To trap the two-phase mixture in the void fraction section, three quick closing valves are used. Two normally open valves are used for controlling

fluid movement at the inlet and exit of the void fraction section, while a normally closed valve is for controlling the entry of fluid into a bypass line. The quick closing valves are W. E. Anderson Model ABV1DA101 Pneumatic Ball Valves and they exhibit a positive seal when closed and have a closing time of 0.03 seconds. When the valves are triggered, the two normally open valves close and the normally closed valve opens simultaneously. In this manner, a two-phase sample is trapped in the void fraction section while the air-water mixture is allowed to continue flowing through the bypass line. Backflow from the mainline into the exit of the bypass line is prevented through the use of a check valve. The experimental procedure of measuring the void fraction with this experimental setup is also discussed in [64]. The uncertainties associated to the measured void fraction results are estimated to be between ±1.25% and ±4.16%.

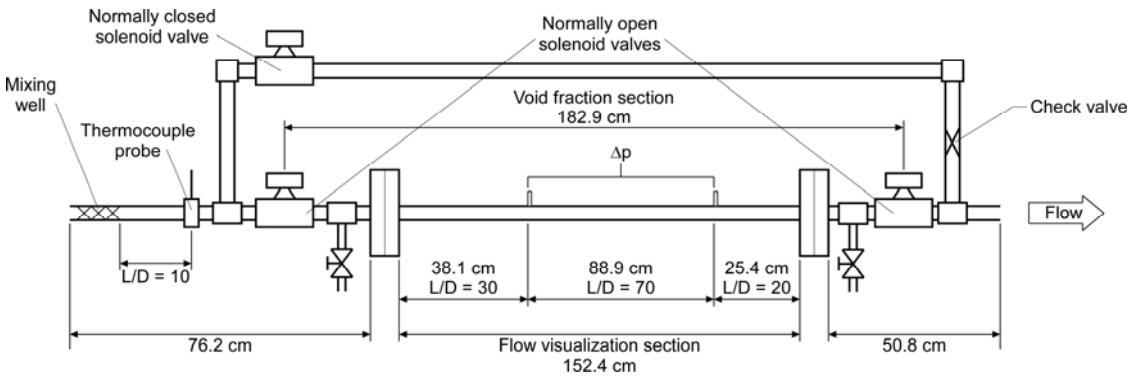

Fig. 9. Test section for flow visualization and void fraction.

Flow Patterns

Flow patterns in horizontal and upward inclined pipes

The various interpretations accorded to the multitude of flow patterns by different investigators are subjective; and no uniform procedure exists at present for describing and classifying them. In this study, the flow pattern identification for the experimental data was based on the procedures suggested by Taitel and Dukler [65], and Kim and Ghajar [61]; and visual observations as deemed appropriate. All observations for the flow pattern judgments were made at the clear polycarbonate observation sections before and after the stainless steel test section (see Fig. 7). By fixing the water flow rate, flow patterns were observed by varying air flow rates. Flow pattern data were obtained at isothermal condition with the pipe in horizontal position and at 2°, 5°, and 7° inclined positions. These experimental data were plotted and compared using their corresponding values of Re_{SG} and Re_{SL}, and the flow patterns. Representative digital images of each flow pattern were taken using a Nikon D50 digital camera with Nikkor 50mm f/1.8D lens. Flow patterns that can be observed in horizontal two-phase flow are illustrated in Fig. 10. The flow map for horizontal flow with the representative

photographs of the various flow patterns is shown in Fig. 11. The various flow patterns for horizontal flow depicted in Fig. 11 show the capability of our experimental setup to cover multitude of flow patterns. The shaded regions represent the transition boundaries of the observed flow patterns.

The influence of small inclination angles of 2°, 5°, and 7° on the observed flow patterns is shown in Fig. 12. As shown in this figure, the flow pattern transition boundaries for horizontal flow were found to be quite different from the flow pattern transition boundaries for inclined flow when slight inclinations of 2°, 5°, and 7° were introduced. The changes in the flow pattern transition boundaries from horizontal to slightly inclined flow are the transition boundaries for stratified flow and slug/wavy flow. When the pipe was inclined from horizontal to slight inclination angles of 2°, 5°, and 7°, the stratified flow region was replaced by slug flow and slug/wavy flow for $Re_{SG} < 4000$ and $4000 < Re_{SG} < 10000$, respectively. Other shifts in the flow pattern transition boundaries were observed in the plug-to-slug boundary and the slug-to-slug/bubbly boundary. In these two cases, the flow pattern transition boundaries were observed to be shifted slightly to the upper left direction as inclination angles were slightly increased from horizontal to 7°. For slightly inclined flow of 2°, 5°, and 7°, there were no drastic changes in the flow pattern transition boundaries.

Table 11. Number of two-phase heat transfer data points measured for different flow patterns and pipe orientations.

Flow patterns	Test section orientation			
	Horizontal	2° inclined	5° inclined	7° inclined
Stratified	20			
Slug	39	44	43	40
Plug	13	14	11	12
Slug/Wavy	7	15	15	15
Wavy	10	8	10	10
Wavy/Annular	22	11	9	9
Slug/Bubbly/Annular	40	47	50	52
Annular	57	45	46	49

For verification of the flow pattern map, flow patterns data from Barnea *et al.* [66] was used and compared with the flow pattern maps for horizontal and 2° inclined pipe. Using flow pattern data from Barnea *et al.* [66] for air-water flow in 25.5 mm diameter horizontal pipe, the data points plotted on the flow map for horizontal flow (see Fig. 11) are illustrated in Fig. 13. The comparison between the data points from Barnea *et al.* [66] and the flow pattern map for horizontal flow showed very satisfactory agreement, especially among the distinctive major flow patterns such as annular, slug and stratified. It should be noted that Barnea *et al.* [66] had successfully compared their horizontal flow pattern data with the flow map proposed by Mandhane *et al.* [67]. In a similar manner, using flow pattern data from Barnea *et al.* [66] for air-water flow in 25.5 mm diameter 2° inclined pipe, the data points plotted on the flow map for 2° inclined flow (see Fig. 12) are illustrated in Fig. 14. The comparison between the data points from Barnea *et al.* [66] and the flow pattern map for 2° inclined flow also showed very satisfactory agreement.

Although the flow patterns may have similar names for both horizontal and inclined flow; that does not mean that the flow patterns in the inclined positions have identical

characteristics of the comparable flow patterns in the horizontal position. For example, it was observed that the slug flow patterns in the inclined positions of 5° and 7° have reverse flow between slugs due to the gravitational force, which can have a significant effect on the heat transfer. To understand the influence of flow patterns on heat transfer, systematic measurement of heat transfer data were conducted. Table 11 and Fig. 15 illustrate the number of two-phase heat transfer data points systematically measured for different flow patterns and test section orientations. Heat transfer data at low air and water flow rates ($Re_{SG} < 500$ and $Re_{SL} < 700$) were not collected. At such low air and water flow rates, there exists the possibility of local boiling or dry-out which could potentially damage the heated test section.

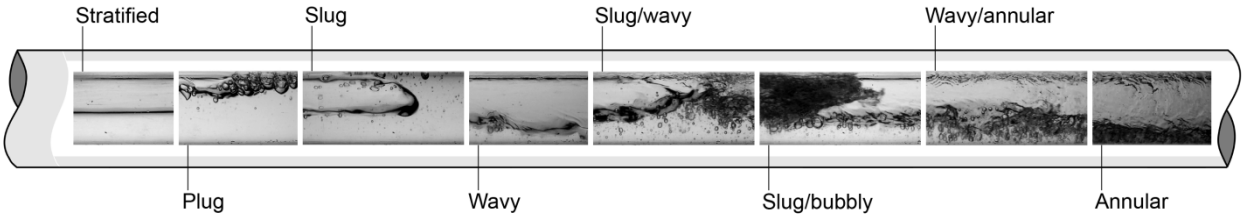

Fig. 10. Flow patterns in horizontal two-phase flow.

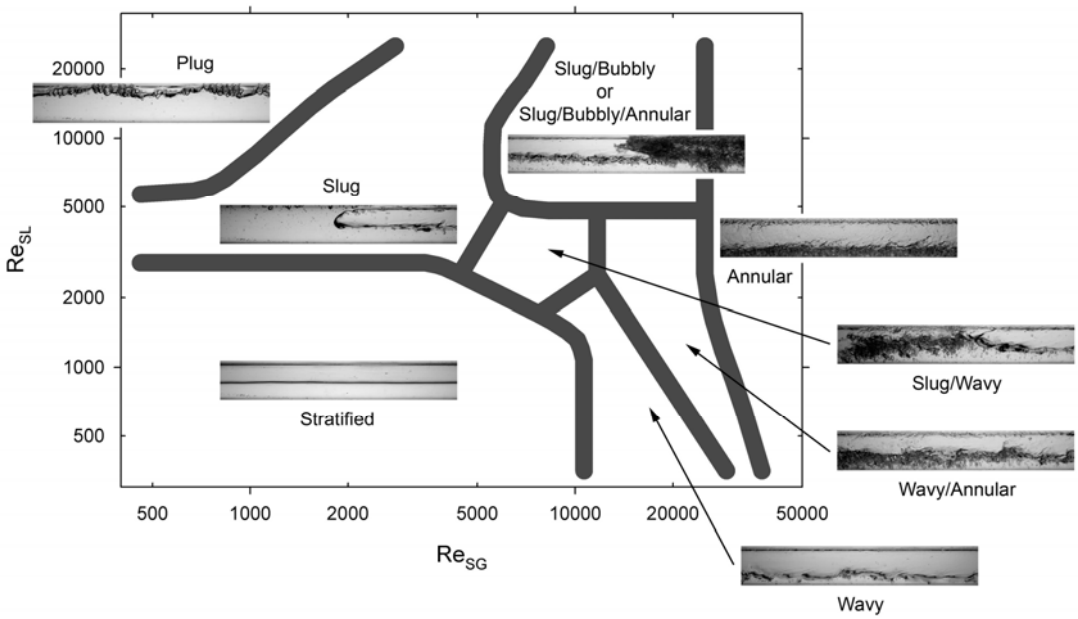

Fig. 11. Flow map for horizontal flow with representative photographs of flow patterns.

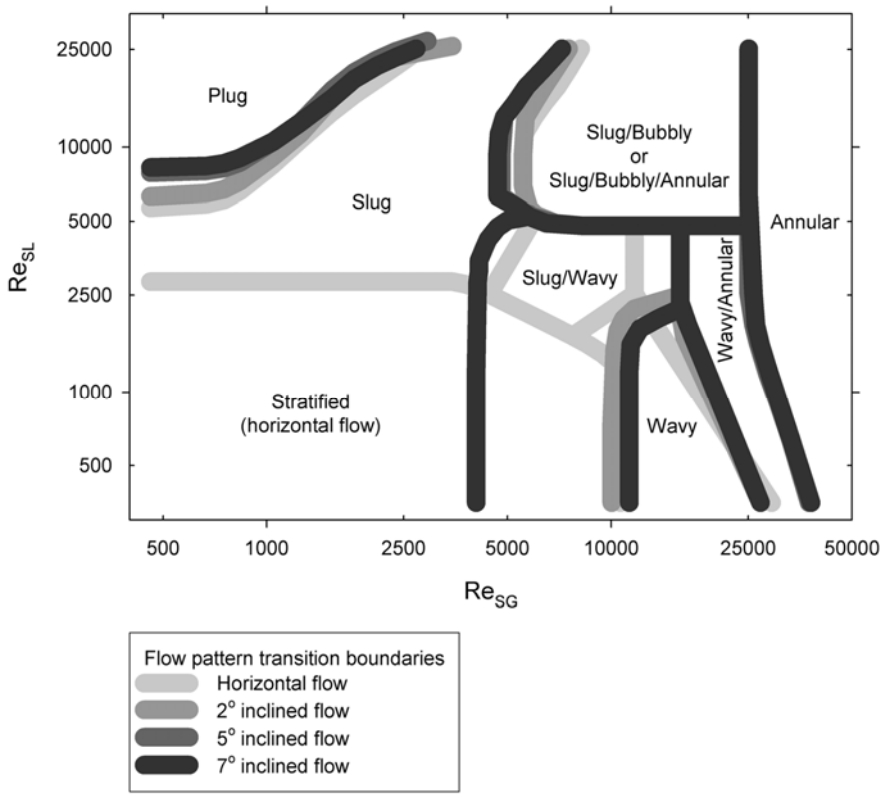

Fig. 12. Change of flow pattern transition boundaries as pipe inclined from horizontal position.

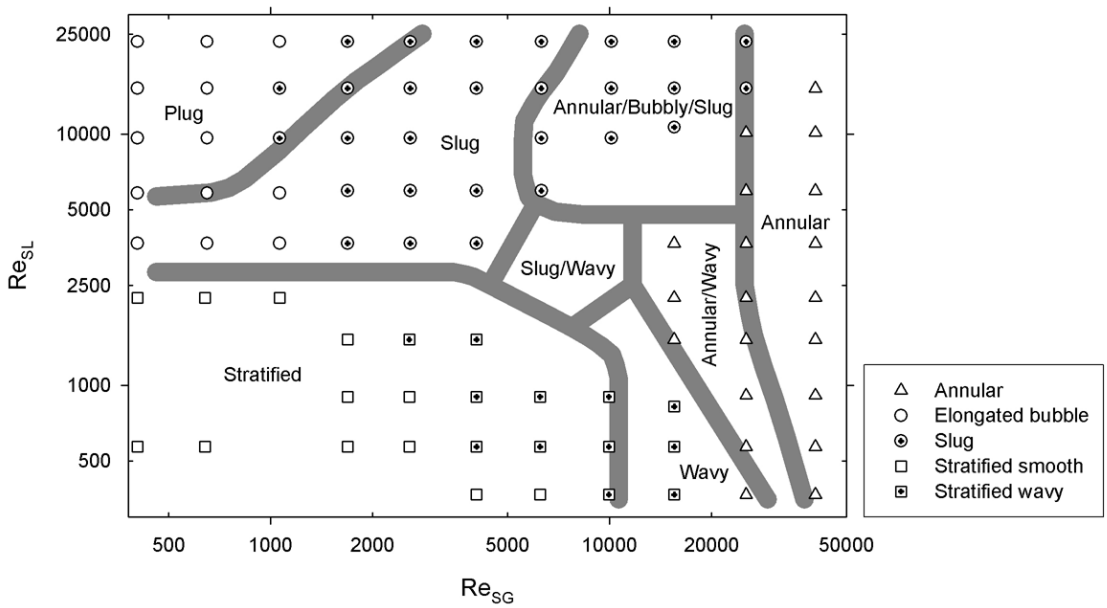

Fig. 13. Flow patterns data points from Barnea *et al.* [66] plotted on the flow map for horizontal flow (see Fig. 11).

Flow patterns in vertical pipes

Flow patterns in upward vertical two-phase air-water flow were conducted at isothermal condition using the robust experimental setup capable for pipe orientation from downward vertical to upward vertical. The experimental setup is equipped for measuring heat transfer, pressure drop, void fraction, and also conducting flow visualization in air-water flow for all major flow patterns and inclination angles, from 0° (horizontal) to ±90° (vertical). All observations for the flow pattern judgments were made at the flow visualization section (see Fig. 9). By fixing the water flow rate, flow patterns were observed by varying air flow rates. Using visual observation and digital photography, distinctive flow patterns were recognized and transition boundaries between flow patterns were determined. The five distinctive major flow patterns observed in the upward vertical two-phase flow are dispersed bubble, slug, churn, froth, and annular. Based on the experimentally documented flow patterns and flow pattern transition boundaries, the two-phase flow pattern map for the upward vertical pipe was delineated. The flow map for vertical flow with the representative photographs of the various flow patterns are shown in Fig. 16. Flow patterns that can be observed in upward vertical two-phase flow are illustrated in Fig. 17. The technique for obtaining the digital images was similar to that employed for horizontal pipe using a Nikon D50 digital camera with Nikkor 50mm f/1.8D lens.

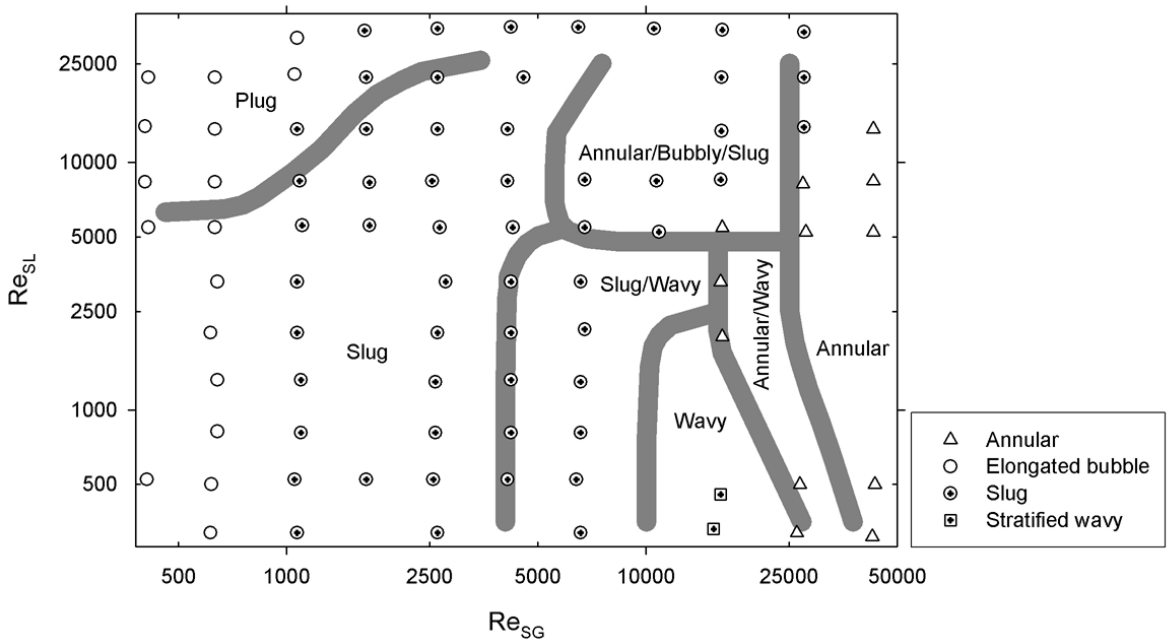

Fig. 14. Flow patterns data points from Barnea *et al.* [66] plotted on the flow map for 2° inclined flow (see Fig. 12).

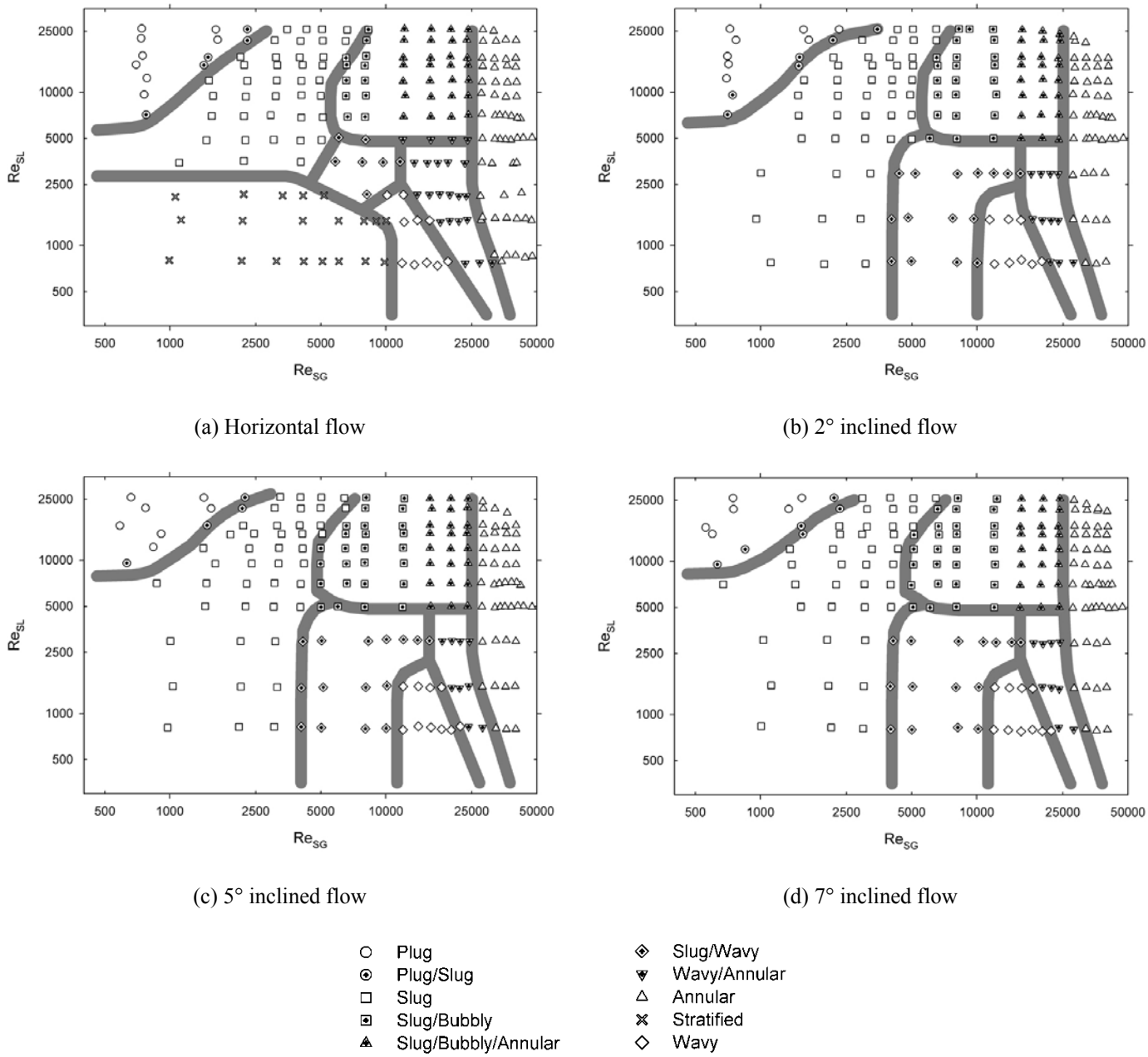

(a) Horizontal flow

(b) 2° inclined flow

(c) 5° inclined flow

(d) 7° inclined flow

Fig. 15. Flow maps for horizontal, 2°, 5°, and 7° inclined flows with distribution of heat transfer data collected.

The slug-churn and churn-annular transition boundaries in this experimental study were compared with correlations available in the literature. The correlation suggested by Wallis [68] is widely used and can be written as

$$V_{SL}^{*1/2} + mV_{SG}^{*1/2} = C \tag{26}$$

where the dimensionless superficial velocities for gas and liquid are expressed as

$$V_{SG}^{*} = V_{SG}\rho_G^{1/2}[gD(\rho_L - \rho_G)]^{-1/2} \tag{26a}$$

and

$$V_{SL}^{*} = V_{SL}\rho_L^{1/2}[gD(\rho_L - \rho_G)]^{-1/2} \tag{26b}$$

In Wallis' original expression of Eq. (26), the values of the dimensionless parameters are $C = m = 1$ [68]. Equation (26) may be treated as an empirical correlation where the parameters C and m depend on the flow conditions at the inlet and outlet as well as geometry. The parameters, C and m, vary approximately within the $0.7 \le C \le 1.0$ and $0.8 \le m \le 1.0$ ranges [25]. McQuillan and Whalley [69] applied Wallis' correlation, Eq. (26), and showed generally good agreement with experimental flow pattern data. The comparison of the experimentally documented slug-churn transition with Eq. (26) is listed in Table 12 and illustrated in Fig. 16. The agreement between the experimental data and Eq. (26), with $C = 0.94$ and $m = 1.0$, is satisfactory and the percentage error is within 6%, see Table 12. At the churn-annular transition, the experimental data was compared with the results from McQuillan and Whalley [69], and agreement is also generally good, see Fig. 16.

Table 12. Comparison of experimental data with Eq. (26), for the slug-churn transition.

V_{SL} [m s^{-1}]	V_{SG} [m s^{-1}]		Error [%]
	Experimental	Eq. (26) ‡	
0.080	1.02	0.975	−4.37
0.165	0.90	0.873	−3.06
0.310	0.70	0.717	2.44
0.460	0.53	0.560	5.73
0.600	0.42	0.417	−0.69

‡ $C = 0.94$ and $m = 1$

Experimental Results of Void Fraction in Upward Vertical Flow

The experimental results of void fraction in upward vertical flow were measured from the test section for flow visualization and void fraction illustrated in Fig. 9. The variation of void fraction with gas mass flow rate for vertical pipe flow is shown in Fig. 18. As liquid mass flow rate increases, the increase in liquid holdup cause the void fraction versus gas mass flow rate curves shift lower. On Fig. 18, the groupings of various flow patterns on the variation of void fraction with gas mass flow rate curves

are shown. Slug flow is confined to low-range gas mass flow rate with $0.25 < \alpha < 0.72$, while churn and froth flows are found in mid-range gas mass flow rate. At any given gas mass flow rate, churn flow has higher void fraction than froth flow. Annular flow is in the high gas mass flow rate region with $0.72 < \alpha < 0.90$. The range of void fraction values observed in the present study for different flow patterns in upward vertical flow is listed in Table 13.

.

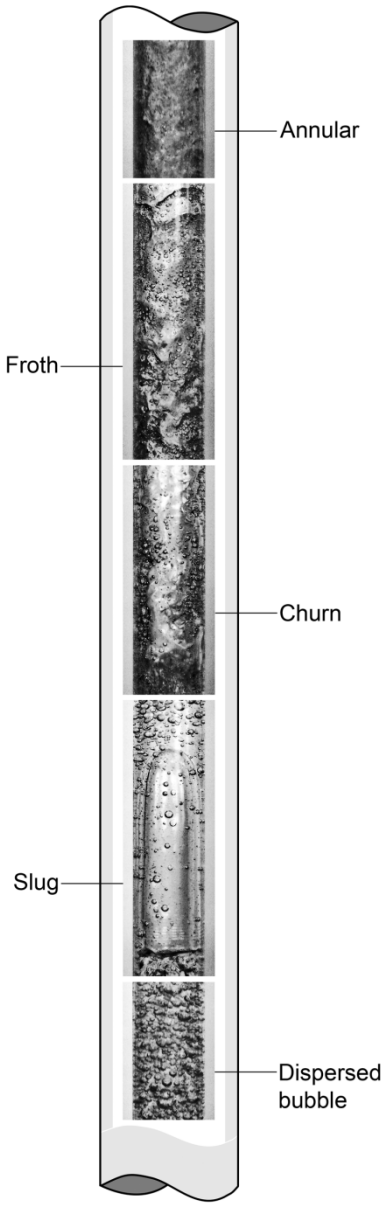

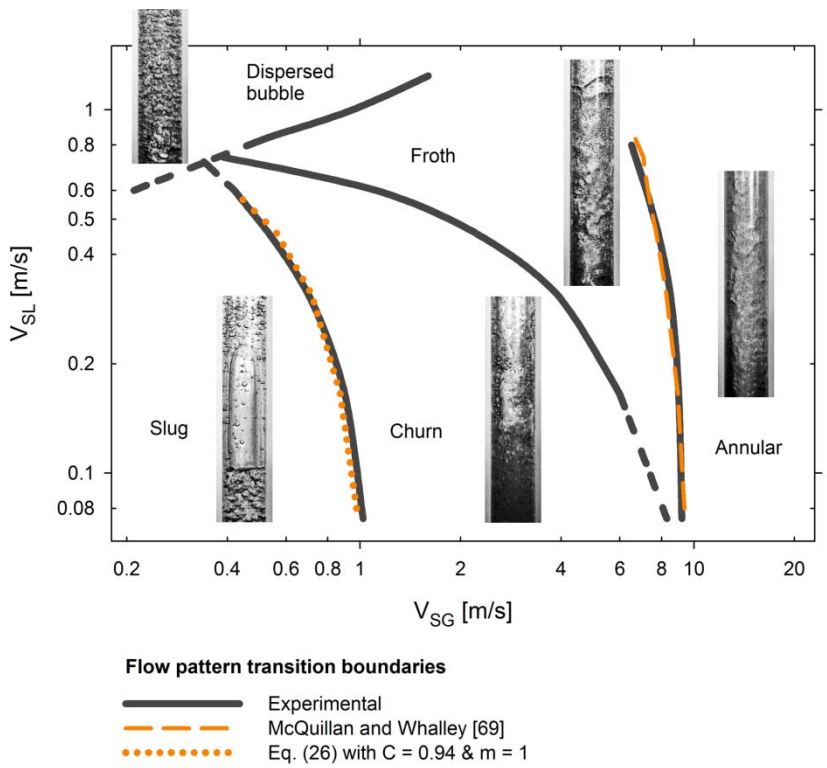

Fig. 16. Flow map for vertical flow with representative photographs of flow patterns.

Fig. 17. Flow patterns in upward vertical two-phase flow.

Table 13. Range of void fraction values for different flow patterns.

Flow pattern	Range of void fraction
Dispersed bubble	0.16 to 0.48
Slug	0.25 to 0.69
Churn	0.35 to 0.77
Froth	0.32 to 0.78
Annular	0.72 to 0.90

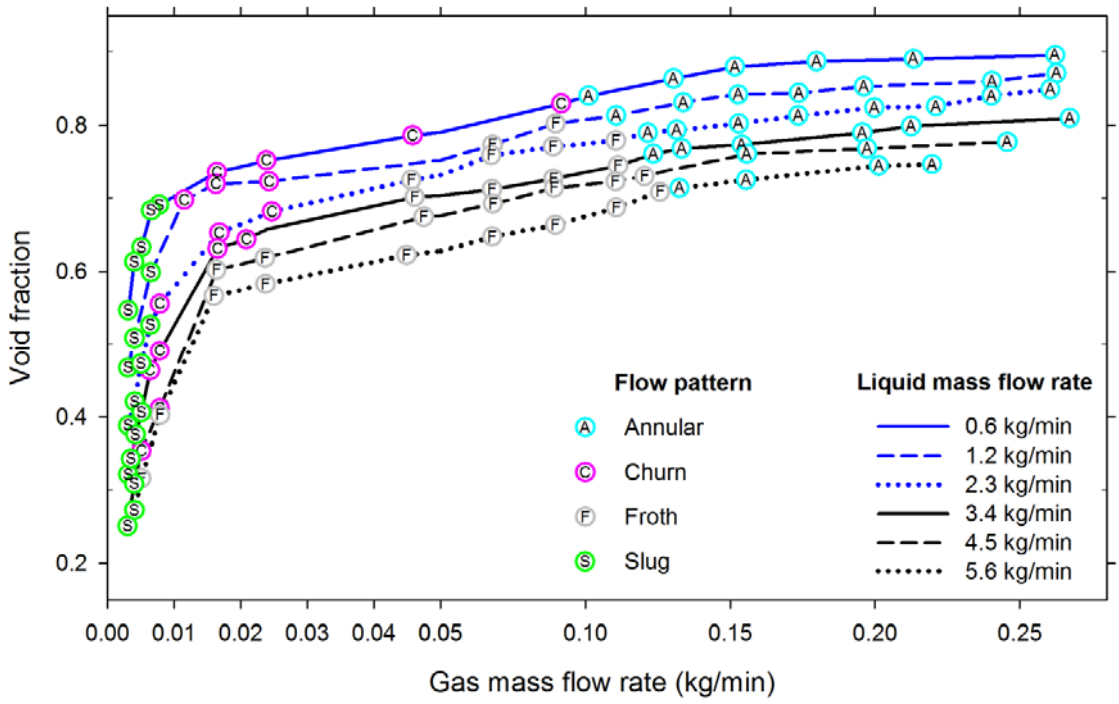

Fig. 18. Variation of void fraction with gas mass flow rate for vertical pipe flow.

Systematic Investigation on Two-Phase Gas-Liquid Flow Heat Transfer in Horizontal and Slightly Upward Inclined Pipes

In this section, an overview of the different trends that have been observed in the heat transfer behavior of the two-phase air-water flow in horizontal and inclined pipes for various flow patterns is presented. The non-boiling two-phase heat transfer data were obtained by systematically varying the air and water flow rates and the pipe inclination angle. The summary of the experimental conditions and measured heat transfer coefficients are tabulated in Table 14. Detailed discussions on the complete experimental results are documented by Ghajar and Tang [57].

Figures 19 and 20 provide an overview of the pronounced influence of the flow pattern, superficial liquid Reynolds number (water flow rate) and superficial gas

Reynolds number (air flow rate) on the two-phase heat transfer coefficient in horizontal flow. The results presented in Fig. 19 clearly show that two-phase heat transfer coefficient is strongly influenced by the superficial liquid Reynolds number (Re_{SL}). As shown in Fig. 19, the heat transfer coefficient increases proportionally as superficial liquid Reynolds number (Re_{SL}) increases. In addition, for a fixed Re_{SL}, the two-phase heat transfer coefficient is also influenced by the superficial gas Reynolds number (Re_{SG}) and each flow pattern shows its own distinguished heat transfer trend as shown in Fig. 20. Typically, heat transfer increases at low Re_{SG} (the regime of plug flow), and then slightly decreases at the mid range of Re_{SG} (the regime of slug and slug-type transitional flows), and increases again at the high Re_{SG} (the regime of annular flow).

Table 14. Summary of experimental conditions and measured two-phase heat transfer data.

	Test section orientation			
	Horizontal	**2° inclined**	**5° inclined**	**7° inclined**
No. of data points	208	184	184	187
Re_{SL} range	740–26100	750–25900	780–25900	770–26000
Re_{SG} range	700–47600	700–47500	590–47500	560–47200
Heat flux range [W m^{-2}]	1860–10800	2820–10800	2900–10800	2600–10900
$h_{TP_{EXP}}$ range [W m^{-2} K^{-1}]	101–5457	242–5140	286–5507	364–5701

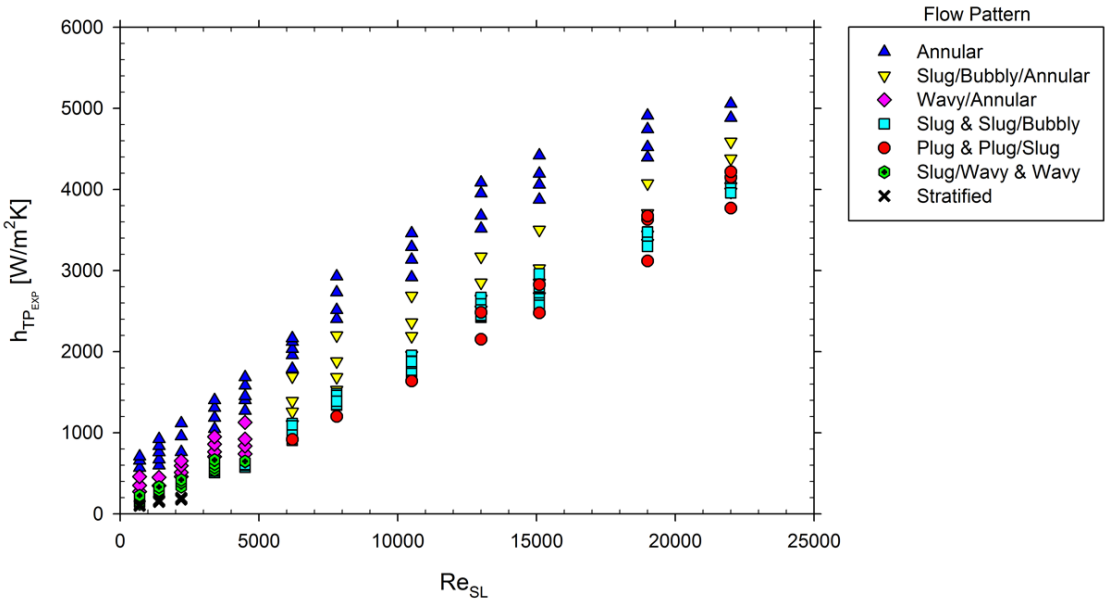

Fig. 19. Variation of two-phase heat transfer coefficient with superficial liquid Reynolds number in horizontal flow.

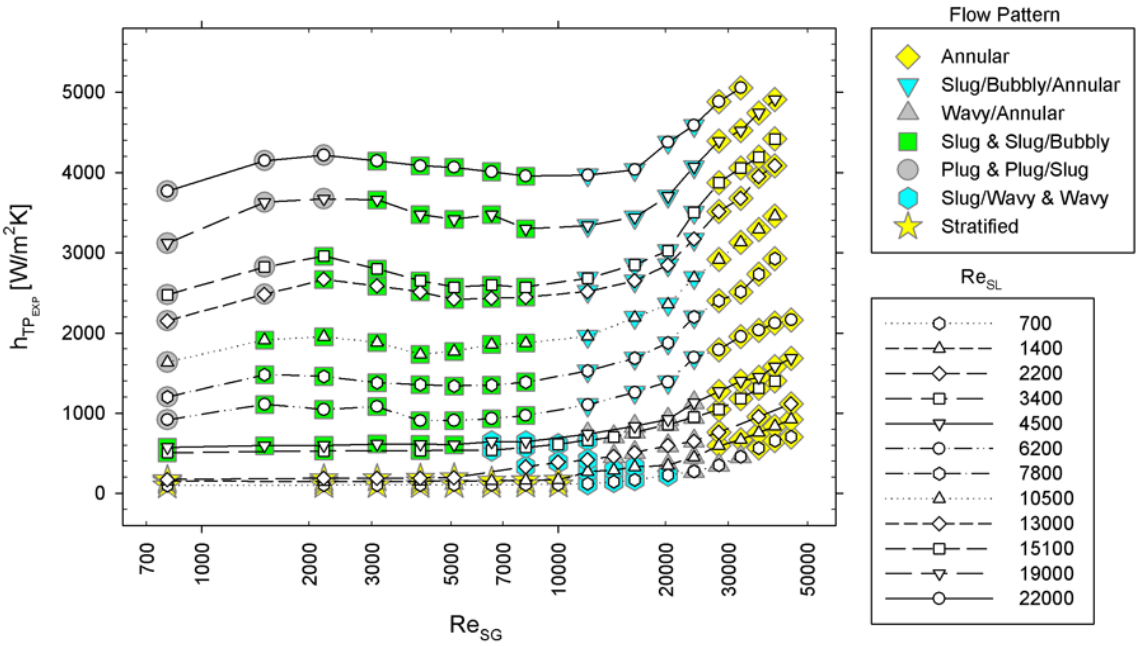

Fig. 20. Variation of two-phase heat transfer coefficient with superficial gas Reynolds number in horizontal flow.

Comparison of General Heat Transfer Correlation with Experimental Results for Various Flow Patterns and Pipe Inclinations

The two-phase heat transfer correlation, Eq. (21) was validated with a total of 763 experimental data points for different flow patterns in horizontal and slightly inclined air-water two-phase pipe flows [56, 58, 59]. Equation (21), performed relatively well by predicting over 85% of the experimental data points to within ±30% for 0°, 2°, 5°, and 7° pipe orientations. Recently, Franca *et al.* [70] compared their mechanistic model developed for convective heat transfer in gas-liquid intermittent (slug) flows with the general heat transfer correlation proposed in this study. For void fraction, Franca *et al.* [70] used their own experimental data which was obtained for air-water flow in a 15 m long, 25.4 mm inside diameter copper pipe. When comparing their mechanistic model with Eq. (21), the agreement is within ±15%, which is considered to be excellent.

However, when comparing the heat transfer correlation, Eq. (21), with data from vertical pipes and different gas-liquid combinations, Eq. (21) has shown some inadequacy in its performance. Equation (21) was validated with 986 experimental data points for different flow patterns, inclination angles, and gas-liquid combinations. The 986 experimental data points were compiled from various sources with different experimental facilities (see Table 15) with a wide range of superficial gas and liquid Reynolds numbers ($750 \leq Re_{SL} \leq 127000$ and $14 \leq Re_{SG} \leq 209000$) and inclination angles ($0° \leq \theta \leq 90°$). Figure 21 shows the comparison of Eq. (21), with all 986

experimental data points for different inclination angles and gas-liquid combinations. Figure 21 shows that Eq. (21) performed well for two-phase flow with heat transfer coefficient between 1000 W m^{-2} K^{-1} and 5000 W m^{-2} K^{-1}. However, Eq. (21) has shown some inadequacy in predicting two-phase flow with heat transfer coefficients below 1000 W m^{-2} K^{-1} and above 5000 W m^{-2} K^{-1}. Overall, Eq. (21) successfully predicted 83% of the 986 experimental data points within ±30% agreement (see Table 15). The results shown in Table 15 and Fig. 21 prompted further investigation and improvements were made on Eq. (21).

Table 15. Results of the predictions for 986 experimental heat transfer data points with different gas-liquid combinations and inclination angles by using Eq. (21).

Data set	RMS dev. (%)	No. of data points within ±20%	No. of data points within ±25%	No. of data points within ±30%	Avg. dev. range (%)	Range of parameters			
						Re_{SL}	Re_{SG}	Pr_G / Pr_L	μ_G / μ_L
All 986 data points $0° \le \theta \le 90°$	33.1	649 (66%)	746 (76%)	817 (83%)	−16.9 to 30.8	750 to 127000	14 to 209000	9.99×10^{-3} to 148×10^{-3}	3.64×10^{-3} to 26.3×10^{-3}
Air-water ($\theta = 0°$) 160 data points [57] 16 data points [70]	20.5	111 (63%)	140 (80%)	154 (88%)	−12.6 to 18.6	2100 to 67000	700 to 48000		
Air-water ($\theta = 2°$) 184 data points [57]	24.9	143 (78%)	154 (84%)	168 (91%)	−12.7 to 23.0	750 to 26000	700 to 48000		
Air-water ($\theta = 5°$) 184 data points [57]	43.4	124 (67%)	137 (74%)	150 (82%)	−15.9 to 64.5	780 to 26000	600 to 48000		
Air-water ($\theta = 7°$) 187 data points [57]	44.7	110 (59%)	132 (71%)	149 (80%)	−16.3 to 74.7	770 to 26000	560 to 47000		
Air-water ($\theta = 90°$) 105 data points [40]	25.0	67 (64%)	79 (75%)	85 (81%)	−22.3 to 2.4	4000 to 127000	43 to 154000		
Air-silicone ($\theta = 90°$) 56 data points [41]	5.9	56 (100%)	56 (100%)	56 (100%)	−4.6 to 6.1	8400 to 21000	52 to 42000		
Helium-water ($\theta = 90°$) 50 data points [42]	25.4	22 (44%)	31 (62%)	37 (74%)	−25.9 to 6.9	4000 to 126000	14 to 13000		
Freon 12-water ($\theta = 90°$) 44 data points [42]	39.1	16 (36%)	17 (39%)	18 (41%)	−33.3 to 0	4200 to 55000	860 to 209000		

Values of constant and exponents: $C = 0.82$, $m = 0.08$, $n = 0.39$, $p = 0.03$, $q = 0.01$, and $r = 0.40$.

With the proposed constant and exponents, $C = 0.55$, $m = 0.1$, $n = 0.4$, and $p = q = r = 0.25$, Eq. (24) was successfully validated with a total of 986 experimental data points for different flow patterns, inclination angles, and gas-liquid combinations. The 986 experimental data points were compiled from various sources with different experimental facilities (see Table 16) with a wide range of superficial gas and liquid Reynolds numbers ($750 \le Re_{SL} \le 127000$ and $14 \le Re_{SG} \le 209000$) and inclination angles ($0° \le \theta \le 90°$). As summarized in Table 16, the comparison of the predictions by

the general two-phase heat transfer correlation, Eq. (24), confirmed that the correlation is adequately robust. Of all the 986 experimental data points, Eq. (24) has successfully predicted 90% of the data points within ±25% agreement with the experimental results. Overall, the prediction by Eq. (24) has a root-mean-square deviation of 18.4% from the experimental data.

Figure 22 shows the comparison of the calculated h_{TP} values from the general heat transfer correlation, Eq. (24), with all 986 experimental data points for different inclination angles and gas-liquid combinations. The comparison of the predictions by Eq. (24) with experimental data for air-water horizontal flow is shown in Fig. 23. The results illustrated in Fig. 23 show that the introduction of the flow pattern factor, Eq. (18), into the general heat transfer correlation, Eq. (24), provides the needed capability to handle different flow patterns. Figure 24 shows the comparison of the predictions by Eq. (24) with experimental data for air-water in slightly inclined pipes (2°, 5° and 7°). Finally, as illustrated in Figure 25, the comparison of the predictions by Eq. (24) with experimental data for various gas-liquid combinations in vertical pipes shows that the modified inclination factor (I^*), see Eq. (22), has adequately accounted for the inclination effects.

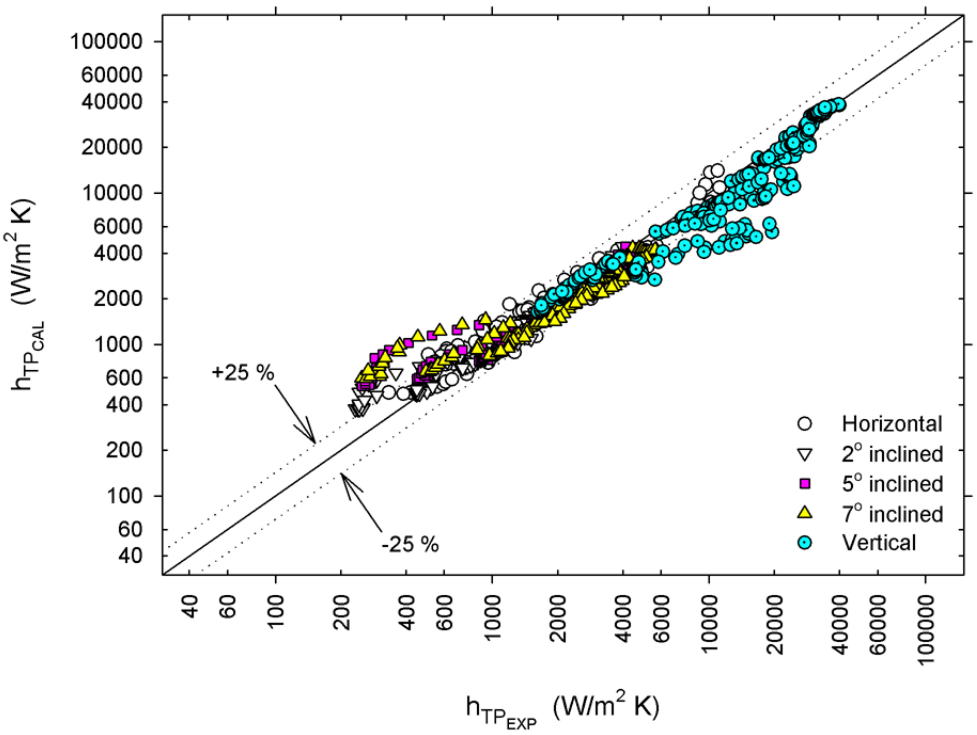

Fig. 21. Comparison of the predictions by Eq. (21) with all 986 experimental data points for different inclination angles and gas-liquid combinations (see Table 15).

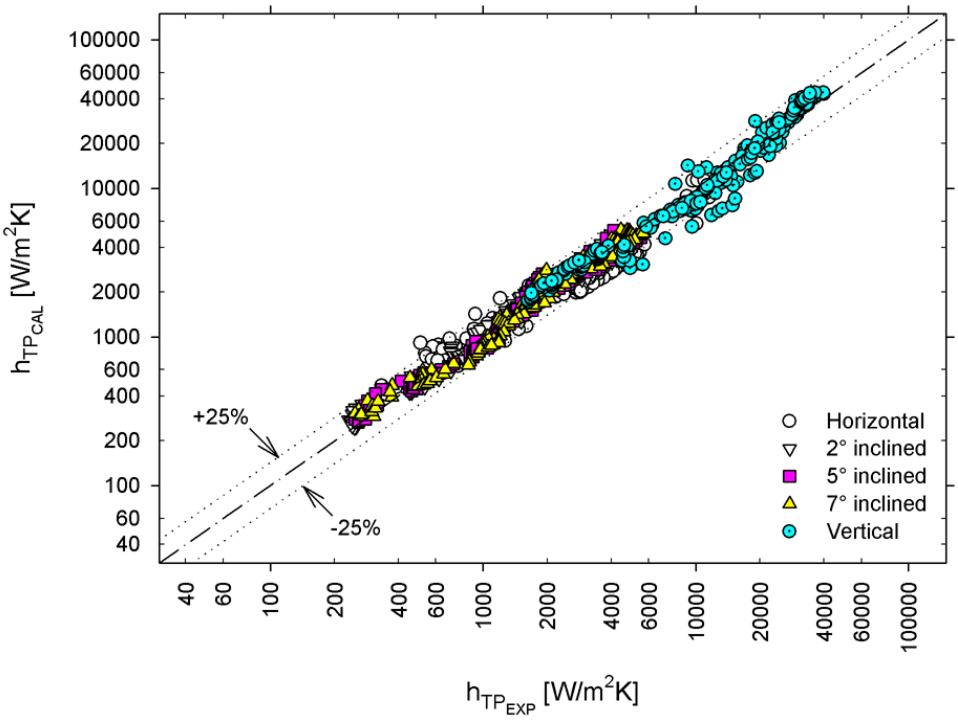

Fig. 22. Comparison of the predictions by Eq. (24) with all 986 experimental data points for different inclination angles and gas-liquid combinations (see Table 16).

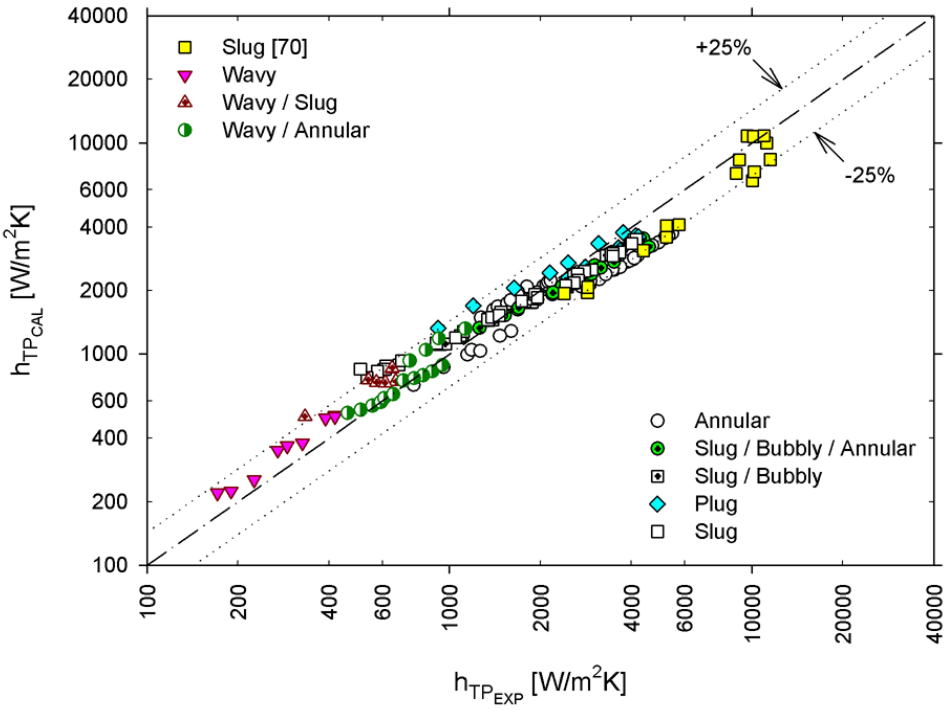

Fig. 23. Comparison of the predictions by Eq. (24) with experimental data for air-water horizontal pipe flow (see Table 16).

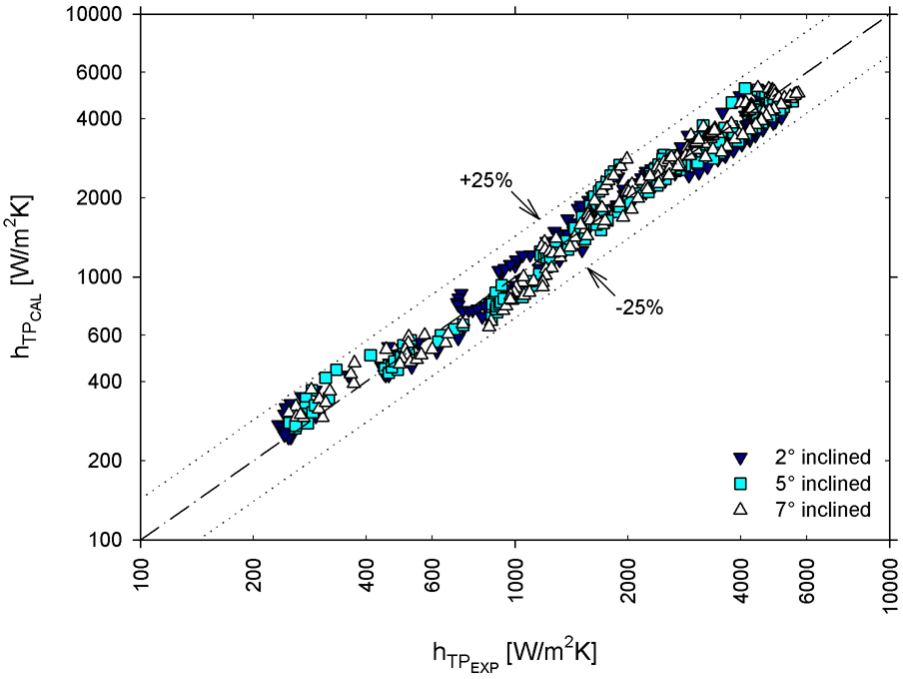

Fig. 24. Comparison of the predictions by Eq. (24) with experimental data for air-water in slightly inclined pipes (see (Table 16).

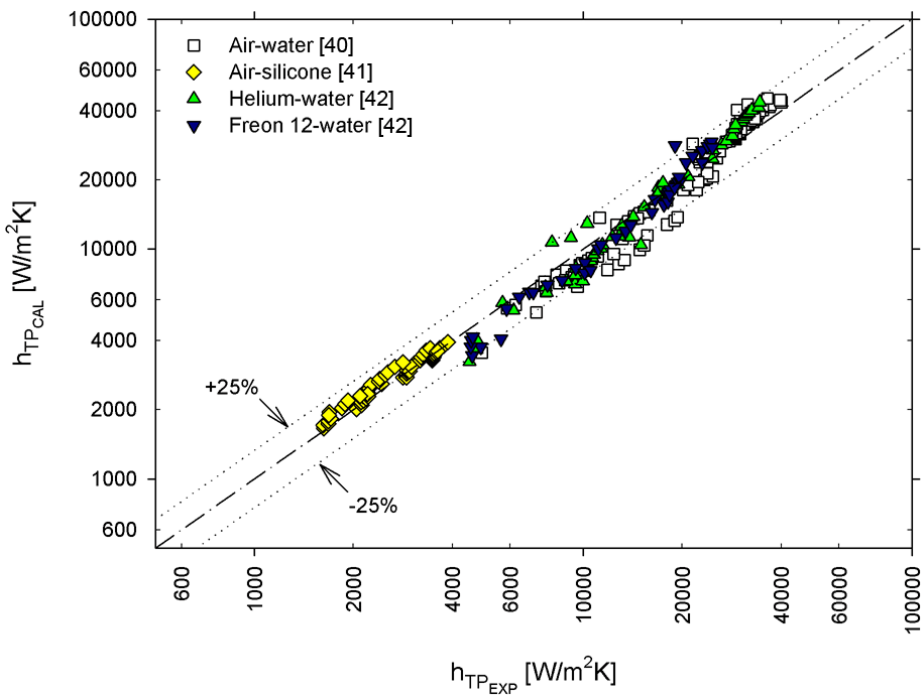

Fig. 25. Comparison of the predictions by Eq. (24) with experimental data for various gas-liquid combinations in vertical pipes (see Table 16).

Table 16. Results of the predictions for 986 experimental heat transfer data points with different gas-liquid combinations and inclination angles by using Eq. (24).

Data set	RMS dev. (%)	No. of data points within ±20%	No. of data points within ±25%	No. of data points within ±30%	Avg. dev. range (%)	Range of parameters			
						Re_{SL}	Re_{SG}	Pr_G / Pr_L	μ_G / μ_L
All 986 data points $0° \le \theta \le 90°$	18.4	793 (80%)	884 (90%)	922 (94%)	−15.3 to 12.5	750 to 127000	14 to 209000	9.99×10^{-3} to 148×10^{-3}	3.64×10^{-3} to 26.3×10^{-3}
Air-water ($\theta = 0°$) 160 data points [57] 16 data points [70]	22.2	127 (72%)	152 (86%)	164 (93%)	−16.2 to 20.4	2100 to 67000	700 to 48000		
Air-water ($\theta = 2°$) 184 data points [57]	13.0	161 (88%)	178 (97%)	184 (100%)	−9.2 to 12.9	750 to 26000	700 to 48000		
Air-water ($\theta = 5°$) 184 data points [57]	12.1	154 (84%)	169 (92%)	174 (95%)	−7.7 to 11.8	780 to 26000	600 to 48000		
Air-water ($\theta = 7°$) 187 data points [57]	12.3	164 (88%)	174 (93%)	176 (94%)	−10.3 to 9.5	770 to 26000	560 to 47000		
Air-water ($\theta = 90°$) 105 data points [40]	23.8	79 (75%)	92 (88%)	95 (90%)	−24.5 to 11.4	4000 to 127000	43 to 154000		
Air-silicone ($\theta = 90°$) 56 data points [41]	10.3	37 (66%)	42 (75%)	47 (84%)	−1.7 to 9.4	8400 to 21000	52 to 42000		
Helium-water ($\theta = 90°$) 50 data points [42]	28.3	41 (82%)	42 (84%)	46 (92%)	−25.9 to 17.6	4000 to 126000	14 to 13000		
Freon 12-water ($\theta = 90°$) 44 data points [42]	29.8	30 (68%)	35 (80%)	36 (82%)	−24.9 to 4.0	4200 to 55000	860 to 209000		

Values of constant and exponents: $C = 0.55$, $m = 0.1$, $n = 0.4$, and $p = q = r = 0.25$.

Practical Illustrations of Using the General Two-Phase Heat Transfer Correlation

The general two-phase heat transfer correlation, Eq. (24), is applicable for estimating heat transfer coefficients for non-boiling two-phase, two-component (liquid and permanent gas) flow in pipes. In this section, three illustrations of using the general two-phase heat transfer correlation, Eq. (24), are discussed. The first illustration is about the application of the correlation on air and gas-oil flow in vertical pipes with gas-to-liquid volume ratio of approximately two. The second illustration is on air and silicone (Dow Corning 200® Fluid, 5 cs) in a vertical pipe with liquid-to-gas volume ratio of approximately ninety. Finally, the third illustration is an application of the correlation on air and water pipe flow in microgravity condition.

Application in air and gas-oil flow

Dorresteijn [71] conducted an experimental study of heat transfer in non-boiling two-phase flow of air and gas-oil through 70-mm diameter vertical tubes. The liquid phase consists of domestic grade gas-oil with kinematic viscosity (ν_L) of 4.7×10^{-6} m^2 s^{-1} and Prandtl number (Pr_L) of approximately 60 [71]. In the conditions at which V_{SG} = 8 m s^{-1}, V_{SL} = 3.16 m s^{-1}, ρ_G = 2.5 kg m^{-3}, ρ_L = 835 kg m^{-3}, and α = 0.67, Dorresteijn [71] measured a value of 1.65 for h_{TP}/h_L. The following example calculation illustrates the use of the general two-phase heat transfer correlation, Eq. (24), to predict the h_{TP}/h_L value measured by Dorresteijn [71].

From the measured superficial gas and liquid velocities, and void fraction, the gas and liquid velocities are found to be

$$V_G = \frac{V_{SG}}{\alpha} = 11.9\,\mathrm{m\,s^{-1}} \qquad \text{and} \qquad V_L = \frac{V_{SL}}{1-\alpha} = 9.58\,\mathrm{m\,s^{-1}}$$

The gas and liquid mass flow rates are calculated as

$$\dot{m}_G = \rho_G V_{SG} A = 0.0771\,\mathrm{kg\,s^{-1}} \qquad \text{and} \qquad \dot{m}_L = \rho_L V_{SL} A = 10.2\,\mathrm{kg\,s^{-1}}$$

Using the gas and liquid mass flow rates, the quality is determined to be

$$x = \frac{\dot{m}_G}{\dot{m}_G + \dot{m}_L} = 0.0075$$

Equations (19) and (18) are then used for calculating the flow pattern factor (F_P),

$$F_S = \frac{2}{\pi}\tan^{-1}\left(\sqrt{\frac{\rho_G (V_G - V_L)^2}{gD(\rho_L - \rho_G)}}\right) = 0.0969 \qquad \text{and} \qquad F_P = (1-\alpha) + \alpha F_S^2 = 0.336$$

Using Eqs. (23) and (22), the inclination factor (I^*) for vertical tube (θ = 90°) is calculated to be

$$\mathrm{Eo} = \frac{(\rho_L - \rho_G) g D^2}{\sigma} = 1600 \qquad \text{and} \qquad I^* = 1 + \mathrm{Eo}\left|\sin\theta\right| = 1601$$

The surface tension (σ) of gas-oil is assumed to be 25×10^{-3} N m^{-1}, since the surface tension for live gas-oil at 1380 kPa ranges from 20×10^{-3} to 30×10^{-3} N m^{-1} [72]. Using the general two-phase heat transfer correlation, Eq. (24), the value for h_{TP}/h_L is estimated to be,

$$\frac{h_{TP}}{h_L} = F_P \left[1 + 0.55 \left(\frac{x}{1-x} \right)^{0.1} \left(\frac{1-F_P}{F_P} \right)^{0.4} \left(\frac{Pr_G}{Pr_L} \right)^{0.25} \left(\frac{\mu_L}{\mu_G} \right)^{0.25} \left(I^* \right)^{0.25} \right] = 1.53$$

The Prandtl number (Pr_G) and dynamic viscosity (μ_G) for air are 0.71 and 18.2×10^{-6} kg m^{-1} s^{-1}, respectively. Comparing with the measured value of $h_{TP}/h_L = 1.65$ by Dorresteijn [71], the general two-phase heat transfer correlation, Eq. (24), under-predicted the measured value by 7.3%.

Application in air and silicone flow

Liquid silicone such as the Dow Corning 200® Fluid, 5 cs, is used primarily as an ingredient in cosmetic and personal care products due to its high spreadability, low surface tension (σ = 19.7×10^{-3} N m^{-1}), non-greasy, soft feel and subtle skin lubricity characteristics. A two-phase flow of air and silicone (Dow Corning 200® Fluid, 5 cs) with $\dot{m}_L = 0.907$ kg s^{-1}, $x = 2.08\times10^{-5}$, $\rho_G = 1.19$ kg m^{-3}, $\rho_L = 913$ kg m^{-3}, $\mu_G = 18.4\times10^{-6}$ kg m^{-1} s^{-1}, $\mu_L = 45.7\times10^{-4}$ kg m^{-1} s^{-1}, $\mu_w = 39.8\times10^{-4}$ kg m^{-1} s^{-1}, $Pr_G = 0.71$, $Pr_L = 64$, k_L = 0.117 W m^{-1} K^{-1}, and $\alpha = 0.011$ flows inside an 11.7-mm diameter vertical ($\theta = 90°$) tube. Using the general two-phase heat transfer correlation, Eq. (24), the two-phase heat transfer coefficient for this flow can be estimated.

With known liquid mass flow rate ($\dot{m}_L$) and quality (x), the gas mass flow rate ($\dot{m}_G$) is determined using

$$\dot{m}_G = \frac{x}{1-x}\dot{m}_L = 1.89\times10^{-5} \text{ kg s}^{-1}$$

From the gas and liquid mass flow rates, the superficial gas and liquid velocities can be calculated:

$$V_{SG} = \frac{\dot{m}_G}{\rho_G A} = 0.149 \text{ m s}^{-1} \qquad \text{and} \qquad V_{SL} = \frac{\dot{m}_L}{\rho_L A} = 9.24 \text{ m s}^{-1}$$

Using the superficial velocities and void fraction, the gas and liquid velocities are found to be

$$V_G = \frac{V_{SG}}{\alpha} = 13.5 \text{ m s}^{-1} \qquad \text{and} \qquad V_L = \frac{V_{SL}}{1-\alpha} = 9.34 \text{ m s}^{-1}$$

Equations (19) and (18) are then used for calculating the flow pattern factor (F_P),

$$F_S = \frac{2}{\pi}\tan^{-1}\left(\sqrt{\frac{\rho_G (V_G - V_L)^2}{g D(\rho_L - \rho_G)}} \right) = 0.266 \qquad \text{and} \qquad F_P = (1-\alpha) + \alpha F_S^2 = 0.990$$

Using Eqs. (23) and (22), the inclination factor (I^*) for vertical tube (θ = 90°) is calculated to be

$$\mathrm{Eo} = \frac{(\rho_L - \rho_G)gD^2}{\sigma} = 62.1 \qquad \text{and} \qquad I^* = 1 + \mathrm{Eo}\left|\sin\theta\right| = 63.1$$

Finally, with the general two-phase heat transfer correlation, Eq. (24), the value for h_{TP} is estimated to be,

$$h_{TP} = h_L F_P \left[1 + 0.55\left(\frac{x}{1-x}\right)^{0.1}\left(\frac{1-F_P}{F_P}\right)^{0.4}\left(\frac{Pr_G}{Pr_L}\right)^{0.25}\left(\frac{\mu_L}{\mu_G}\right)^{0.25}\left(I^*\right)^{0.25}\right] = 3550\ \mathrm{W\ m^{-2}\ K^{-1}}$$

When compared with the measured two-phase heat transfer coefficient of 3480 W m^{-2} K^{-1} by Rezkallah [41] in similar flow conditions, the general two-phase heat transfer correlation, Eq. (24), over-predicted the measured value by 2%.

Application in microgravity condition

An air-water slug flow heat transfer coefficient in microgravity condition (less than 1% of earth's normal gravity) was measured by Witte *et al.* [73] in a 25.4-mm diameter horizontal tube. In the conditions at which V_{SG} = 0.3 m s^{-1}, V_{SL} = 0.544 m s^{-1}, ρ_G = 1.16 kg m^{-3}, ρ_L = 997 kg m^{-3}, μ_G = 18.5×10^{-6} kg m^{-1} s^{-1}, μ_L = 85.5×10^{-5} kg m^{-1} s^{-1}, μ_w = 73.9×10^{-5} kg m^{-1} s^{-1}, Pr$_G$ = 0.71, Pr$_L$ = 5.0, k_L = 0.613 W m^{-1} K^{-1} and α = 0.27, Witte *et al.* [73] measured a value of 3169 W m^{-2} K^{-1} for the two-phase heat transfer coefficient (h_{TP}). The following example calculation illustrates the use of the general two-phase heat transfer correlation, Eq. (24), to predict the h_{TP} value measured by Witte *et al.* [73].

From the measured superficial gas and liquid velocities, and void fraction, the gas and liquid velocities are found to be

$$V_G = \frac{V_{SG}}{\alpha} = 1.11\ \mathrm{m\,s^{-1}} \qquad \text{and} \qquad V_L = \frac{V_{SL}}{1-\alpha} = 0.745\ \mathrm{m\,s^{-1}}$$

The gas and liquid mass flow rates are calculated as

$$\dot{m}_G = \rho_G V_{SG} A = 1.76\times10^{-4}\ \mathrm{kg\,s^{-1}} \qquad \text{and} \qquad \dot{m}_L = \rho_L V_{SL} A = 0.275\ \mathrm{kg\,s^{-1}}$$

Using the gas and liquid mass flow rates, the quality is determined to be

$$x = \frac{\dot{m}_G}{\dot{m}_G + \dot{m}_L} = 6.40\times10^{-4}$$

Equations (19) and (18) are then used for calculating the flow pattern factor (F_P),

$$F_S = \frac{2}{\pi}\tan^{-1}\left(\sqrt{\frac{\rho_G\,(V_G - V_L)^2}{g\,D\,(\rho_L - \rho_G)}}\right) = 0.0159 \qquad \text{and} \qquad F_P = (1-\alpha) + \alpha\,F_S^2 = 0.730$$

The inclination factor (I^*) has a value of one in horizontal tube ($\theta = 0$). Thus, using the general two-phase heat transfer correlation, Eq. (24), the value for h_{TP} is estimated to be,

$$h_{TP} = h_L F_P \left[1 + 0.55\left(\frac{x}{1-x}\right)^{0.1}\left(\frac{1-F_P}{F_P}\right)^{0.4}\left(\frac{Pr_G}{Pr_L}\right)^{0.25}\left(\frac{\mu_L}{\mu_G}\right)^{0.25}\left(I^*\right)^{0.25}\right] = 2810\ \text{W m}^{-2}\ \text{K}^{-1}$$

Comparing with the measured two-phase heat transfer coefficient of 3169 W m^{-2} K^{-1} by Witte *et al.*[73], the general two-phase heat transfer correlation, Eq. (24), under-predicted the measured value by 11%. Although the above example showed that Eq. (24) can satisfactorily estimate heat transfer coefficient for one case of two-phase flow under reduced gravity condition, it should be noted that Eq. (24) was not developed to handle reduced gravity conditions. Validation with experimental results needs to be done before the use of Eq. (24) in reduced gravity conditions can be recommended.

Summary

The work documented in this manuscript initiated with the motivation to understand, in both fundamental and industrial applications, the importance of non-boiling two-phase flow heat transfer in pipes. Through the survey of literature and tracing the validity and limitations of the numerous two-phase non-boiling heat transfer correlations that have been published over the past six decades, it was established that there is no single correlation capable of predicting the two-phase flow heat transfer for all fluid combinations in vertical pipes [39].

The results from the literature survey prompted the development of a two-phase non-boiling heat transfer correlation that is robust and applicable to turbulent gas-liquid flow in vertical pipes with different flow patterns and fluid combinations [47]. Since the development of the two-phase non-boiling heat transfer correlation for vertical pipes by Kim *et al.* [47], extensive efforts have been invested in the development of the general two-phase heat transfer correlation, Eq. (24). When compared with experimental data from horizontal, slightly inclined, and vertical pipes with various fluid combinations and flow patterns, the general two-phase heat transfer correlation successfully predicted 90% of the data points within ±25% agreement with the experimental data and has a root-mean-square deviation of 18.4% from the experimental data. In addition, practical illustrations of using the general two-phase heat transfer correlation were also discussed.

In the efforts of investigating non-boiling two-phase flow heat transfer in pipes, significant amount of work has also been done on understanding void fraction. A very extensive comparison of 68 void fraction correlations available in the literature against 2845 experimental data points was conducted by Woldesemayat and Ghajar [10]. From this work an improved void fraction correlation, Eq. (2), was proposed. The improved

void fraction correlation gives noticeable improvements over other correlations when compared with 2845 experimental data points of various pipe sizes, inclinations, and two-phase fluid mixtures from various sources with different experimental facilities. Further scrutiny has also been done specifically for upward vertical two-phase flow on the performances of available void fraction correlations. A database of 1208 experimental data points, for different gas-liquid combinations and pipe diameters, was used for the comparison with void fraction correlations available in the literature. The effort resulted in the categorization of void fraction correlations recommended for specific void fraction ranges in upward vertical two-phase flow. Results of these categorical comparisons would allow the access to correlations with higher accuracies for specific void fraction range of interest.

The overall objective of this on-going research has been to establish a fundamental understanding of two-phase flow in pipes. Although the initial effort has been on the development of heat transfer in non-boiling two-phase flow, the focus now has been expanded to encompass void fraction, flow patterns and even pressure drop in two-phase flow. The direction is certainly toward gaining understanding of the fundamentals in the hydrodynamic and thermal aspects of gas-liquid two-phase flow in pipes of all possible orientations.

Acknowledgements

Sincere thanks are offered to Emerson Micro Motion for generously donating one of the Coriolis flow meters and providing a substantial discount on the other one. Thanks are also due to Mr. Martin Mabry for his assistance in procuring these meters. The authors also thank Mr. Pranav Godbole for his contributions in the experimental part for void fraction and flow patterns as well as the analysis of void fraction correlations in upward vertical two-phase flow [74].

Nomenclature

A	cross sectional area, m^2
C	constant value of the leading coefficient in Eqs. (13), (21) & (24); and parameter of Wallis' correlation, Eq (26), dimensionless
C_0	two-phase distribution coefficient, dimensionless
c	specific heat at constant pressure, J kg^{-1} K^{-1}
D	pipe inside diameter, m
Eo	Eötvös number, dimensionless
F_P	flow pattern factor, Eq. (18), dimensionless
F_S	shape factor, Eq. (19), dimensionless
g	gravitational acceleration, m s^{-2}
h	heat transfer coefficient, W m^{-2} K^{-1}
I	inclination factor, Eq. (20), dimensionless
I^*	modified inclination factor, Eq. (22), dimensionless

K	slip ratio, V_G/V_L, dimensionless
k	thermal conductivity, W m^{-1} K^{-1}
L	length, m
m	constant in Wallis' correlation, Eq. (26), dimensionless
$\dot{m}$	mass flow rate, kg s^{-1}
N_{ST}	number of thermocouple stations, dimensionless
Nu	Nusselt number, hD/k, dimensionless
P	pressure, Pa
Pr	Prandtl number, $c\mu/k$, dimensionless
Q	volumetric flow rate, m^3 s^{-1}
$\dot{q}''$	heat flux, W m^{-2}
Re	Reynolds number, $\rho VD/\mu$, dimensionless
Re_L	*in situ* liquid Reynolds number, Eq. (15), dimensionless
S_L	wetted perimeter, m
T	temperature, K
u_{GM}	drift velocity for gas, m s^{-1}
V	velocity, m s^{-1}
V^*	superficial velocity in Wallis' correlation, Eq. (26), dimensionless
x	flow quality, $\dot{m}_G/(\dot{m}_G+\dot{m}_L)$, dimensionless
z	axial coordinate, m
Δz	element length of each thermocouple station, m

Greek Symbols

α	void fraction, dimensionless
θ	inclination angle, rad.
μ	dynamic viscosity, kg m^{-1} s^{-1}
ν	kinematic viscosity, m^2 s^{-1}
ρ	density, kg m^{-3}
σ	surface tension, N m^{-1}

Subscripts

atm	atmosphere
B	bulk
CAL	calculated
eff	effective
eq	equilibrium state
EXP	experimental
G	gas
k	index of thermocouple station
L	liquid
SG	superficial gas
SL	superficial liquid
sys	system
TP	two-phase
w	wall

Superscripts

m	exponent on the quality ratio term in Eqs. (13), (21) & (24), dimensionless
n	exponent in Eqs. (13), (21) & (24), dimensionless
p	exponent on the Prandtl number ratio term in Eqs. (13), (21) & (24), dimensionless
q	exponent on the viscosity ratio term in Eqs. (13), (21) & (24), dimensionless
r	exponent on the inclination factor in Eqs. (21) & (24), dimensionless

Diacritical Marks

$-$	local mean
$\sim$	non-dimensionalized

References

[1] K. C. Shiu and H. D. Beggs, "Predicting temperatures in flowing oil wells," *Journal of Energy Resources Technology,* vol. 102, pp. 2-11, 1980.

[2] O. V. Trevisan, F. A. Franca, and A. C. Lisboa, "Oil production in offshore fields: An overview of the brazilian technology development program," in *Proceedings of the 1st World Heavy Oil Conference*, Beijing, China, 2006.

[3] E. M. Furuholt, "Multiphase technology: Is it of interest for future field developments?," in *Society of Petroleum Engineers European Petroleum Conference*, London, England, 1988.

[4] G. G. McClaflin and D. L. Whitfill, "Control of paraffin deposition in production operations," *Journal of Petroleum Technology,* vol. 36, pp. 1965-1970, 1984.

[5] H. S. Fogler, "Paraffin research," *Porous Media Research Group,* Website: <sitemaker.umich.edu/sfogler/paraffin_deposition>, Retrieved Sep. 29, 2009.

[6] P. Singh, R. Venkatesan, H. S. Fogler, and N. Nagarajan, "Formation and aging of incipient thin film wax-oil gels," *AIChE Journal,* vol. 46, pp. 1059-1074, 2000.

[7] G. P. Celata, A. Chiaradia, M. Cumo, and F. D'Annibale, "Heat transfer enhancement by air injection in upward heated mixed-convection flow of water," *International Journal of Multiphase Flow,* vol. 25, pp. 1033-1052, 1999.

[8] L. B. Fore, L. C. Witte, and J. B. McQuillen, "Heat transfer to annular gas-liquid mixtures at reduced gravity," *Journal of Thermophysics and Heat Transfer,* vol. 10, pp. 633-639, 1996.

[9] L. B. Fore, L. C. Witte, and J. B. McQuillen, "Heat transfer to two-phase slug flows under reduced-gravity conditions," *International Journal of Multiphase Flow,* vol. 23, pp. 301-311, 1997.

[10] M. A. Woldesemayat and A. J. Ghajar, "Comparison of void fraction correlations for different flow patterns in horizontal and upward inclined pipes," *International Journal of Multiphase Flow,* vol. 33, pp. 347-370, 2007.

[11] B. A. Eaton, "The prediction of flow patterns, liquid holdup and pressure losses occurring during continuous two-phase flow in horizontal pipelines," Ph.D. thesis, University of Texas, Austin, Texas, 1966.

[12] H. D. Beggs, "An experimental study of two phase flow in inclined pipes," Ph.D. thesis, University of Tulsa, Tulsa, Oklahoma, 1972.

[13] P. L. Spedding and V. T. Nguyen, "Data on holdup, pressure loss and flow patterns for two-phase air-water flow in an inclined pipe," Eng. Report 122, University of Auckland, Auckland, New Zealand, 1976.

[14] H. Mukherjee, "An experimental study of inclined two-phase flow," Ph.D. thesis, University of Tulsa, Tulsa, Oklahoma, 1979.

[15] K. Minami and J. P. Brill, "Liquid holdup in wet-gas pipelines," *SPE Production Engineering,* vol. 2, pp. 36-44, 1987.

[16] F. Franca and R. T. Lahey Jr., "The use of drift-flux techniques for the analysis of horizontal two-phase flows," *International Journal of Multiphase Flow,* vol. 18, pp. 787-801, 1992.

[17] G. H. Abdul-Majeed, "Liquid holdup in horizontal two-phase gas-liquid flow," *Journal of Petroleum Science and Engineering,* vol. 15, pp. 271-280, 1996.

[18] M. Sujumnong, "Heat transfer, pressure drop and void fraction in two-phase, two component flow in a vertical tube," Ph.D. thesis, University of Manitoba, Winnipeg, Manitoba, Canada, 1998.

[19] S. Morooka, T. Ishizuka, M. IIzuka, and K. Yoshimura, "Experimental study on void fraction in a simulated bwr fuel assembly (evaluation of cross-sectional averaged void fraction)," *Nuclear Engineering and Design,* vol. 114, pp. 91-98, 1989.

[20] G. E. Dix, "Vapor void fractions for forced convection with subcooled boiling at low flow rates," Ph.D. thesis, University of California, Berkeley, California, 1971.

[21] S. Z. Rouhani and E. Axelsson, "Calculation of void volume fraction in the subcooled and quality boiling regions," *International Journal of Heat and Mass Transfer,* vol. 13, pp. 383-393, 1970.

[22] G. A. Hughmark, "Holdup in gas-liquid flow," *Chemical Engineering Progress,* vol. 58, pp. 62-65, 1962.

[23] A. Premoli, D. Francesco, and A. Prima, "An empirical correlation for evaluating two-phase mixture density under adiabatic conditions," in *European Two-Phase Flow Group Meeting*, Milan, Italy, 1970.

[24] A. I. Filimonov, M. M. Przhizhalovski, E. P. Dik, and J. N. Petrova, "The driving head in pipes with a free interface in the pressure range from 17 to 180 atm," *Teploenergetika,* vol. 4, pp. 22-26, 1957.

[25] S. M. Ghiaasiaan, *Two-phase flow, boiling, and condensation*. New York: Cambridge University Press, 2008.

[26] D. J. Nicklin, J. O. Wilkes, and J. F. Davidson, "Two-phase flow in vertical tubes," *Chemical Engineering Research and Design,* vol. 40, pp. 61-68, 1962.

[27] J. Schmidt, H. Giesbrecht, and C. W. M. van der Geld, "Phase and velocity distributions in vertically upward high-viscosity two-phase flow," *International Journal of Multiphase Flow,* vol. 34, pp. 363-374, 2008.

[28] R. Chokshi, "Prediction of pressure drop and liquid hold up in vertical two-phase flow through large diameter tubing," Ph.D. thesis, University of Tulsa, Tulsa, Oklahoma, 1994.

[29] R. C. Fernandes, "Experimental and theoretical studies of isothermal upward gas-liquid flows in vertical tubes," Ph.D. thesis, University of Houston, Houston, Texas, 1981.

[30] O. Oshinowo, "Two-phase flow in a vertical tube coil," Ph.D. thesis, University of Toronto, Toronto, Canada, 1971.

[31] H. S. Isbin, N. C. Shear, and K. C. Eddy, "Void fractions in steam water two-phase flow," *AIChE Journal,* vol. 3, pp. 136-142, 1957.

[32] H. Nishino and Y. Yamazaki, "A new method of evaluating steam volume fractions in boiling systems," *Journal of Society of Atomic Energy Japan,* vol. 5, pp. 39-59, 1963.

[33] A. L. Guzhov, V. A. Mamayev, and G. E. Odishariya, "A study of transportation in gas liquid systems," in *10th International Gas Union Conference*, Hamburg, Germany, 1967.

[34] R. H. Bonnecaze, W. Erskine, and E. J. Greskovich, "Holdup and pressure drop for two-phase slug flow in inclined pipelines," *AIChE Journal,* vol. 17, pp. 1109-1113, 1971.

[35] M. Ishii, "One-dimensional drift-flux model and constitutive equations for relative motion between phases in various two-phase flow regimes," Argonne National Lab. Report, ANL-77-47, 1977.

[36] K. H. Sun, R. B. Duffey, and C. M. Peng, "A thermal-hydraulic analysis of core uncovery," in *Proceedings of the 19th National Heat Transfer Conference, Experimental and Analytical Modeling of LWR Safety Experiments*, Orlando, Florida, 1980, pp. 1-10

[37] S. L. Kokal and J. F. Stanislav, "An experimental study of two-phase flow in slightly inclined pipes--ii. Liquid holdup and pressure drop," *Chemical Engineering Science,* vol. 44, pp. 681-693, 1989.

[38] K. Takeuchi, M. Y. Young, and L. E. Hochreiter, "Generalized drift flux correlation for vertical flow," *Nuclear Science and Engineering,* vol. 112, pp. 170-180, 1992.

[39] D. Kim, A. J. Ghajar, R. L. Dougherty, and V. K. Ryali, "Comparison of 20 two-phase heat transfer correlations with seven sets of experimental data, including flow pattern and tube inclination effects," *Heat Transfer Engineering,* vol. 20, pp. 15-40, 1999.

[40] M. M. Vijay, "A study of heat transfer in two-phase two-component flow in a vertical tube," Ph.D. thesis, University of Manitoba, Winnipeg, Manitoba, Canada, 1978.

[41] K. S. Rezkallah, "Heat transfer and hydrodynamics in two-phase two-component flow in a vertical tube," Ph.D. thesis, University of Manitoba, Winnipeg, Manitoba, Canada, 1987.

[42] M. A. Aggour, "Hydrodynamics and heat transfer in two-phase two-component flow," Ph.D. thesis, University of Manitoba, Winnipeg, Manitoba, Canada, 1978.

[43] R. H. Pletcher, "An experimental and analytical study of heat transfer and pressure drop in horizontal annular two-phase, two-component flow," Ph.D. thesis, Cornell University, Ithaca, New York, 1966.

[44] C. D. G. King, "Heat transfer and pressure drop for an air-water mixture flowing in a 0.737inch i.D. Horizontal tube," M.S. thesis, University of California, Berkeley, California, 1952.

[45] Y.-C. Chu and B. G. Jones, "Convective heat transfer coefficient studies in upward and downward, vertical, two-phase, non-boiling flows," *AIChE Symposium Series,* vol. 76, pp. 79-90, 1980.

[46] S. R. Ravipudi and T. M. Godbold, "The effect of mass transfer on heat transfer on heat transfer rates for two-phase flow in a vertical pipe," in *Proceedings of the 6th International Heat Transfer Conference*, Toronto, Canada, 1978, pp. 505-510.

[47] D. Kim, A. J. Ghajar, and R. L. Dougherty, "Robust heat transfer correlation for turbulent gas-liquid flow in vertical pipes," *Journal of Thermophysics and Heat Transfer,* vol. 14, pp. 574-578, 2000.

[48] R. F. Knott, R. N. Anderson, A. Acrivos, and E. E. Petersen, "An experimental study of heat transfer to nitrogen-oil mixtures," *Industrial & Engineering Chemistry,* vol. 51, pp. 1369-1372, 1959.

[49] E. N. Sieder and G. E. Tate, "Heat transfer and pressure drop of liquids in tubes," *Industrial & Engineering Chemistry,* vol. 28, pp. 1429-1435, 1936.

[50] A. A. Kudirka, R. J. Grosh, and P. W. McFadden, "Heat transfer in two-phase flow of gas-liquid mixtures," *Industrial & Engineering Chemistry Fundamentals,* vol. 4, pp. 339-344, 1965.

[51] B. W. Martin and G. E. Sims, "Forced convection heat transfer to water with air injection in a rectangular duct," *International Journal of Heat and Mass Transfer,* vol. 14, pp. 1115-1134, 1971.

[52] K. S. Rezkallah and G. E. Sims, "Examination of correlations of mean heat transfer coefficients in two-phase two-component flow in vertical tubes," *AIChE Symposium Series,* vol. 83, pp. 109-114, 1987.

[53] M. M. Shah, "Generalized prediction of heat transfer during two component gas-liquid flow in tubes and other channels," *AIChE Symposium Series,* vol. 77, pp. 140-151, 1981.

[54] D. Chisholm, "Research note: Void fraction during two-phase flow," *Journal of Mechanical Engineering Science,* vol. 15, pp. 235-236, 1973.

[55] A. J. Ghajar and J. Kim, "A non-boiling two-phase flow heat transfer correlation for different flow patterns and pipe inclination angles," in *Proceedings of the 2005 ASME Summer Heat Transfer Conference*, San Francisco, CA, 2005.

[56] J. Kim and A. J. Ghajar, "A general heat transfer correlation for non-boiling gas-liquid flow with different flow patterns in horizontal pipes," *International Journal of Multiphase Flow,* vol. 32, pp. 447-465, 2006.

[57] A. J. Ghajar and C. C. Tang, "Heat transfer measurements, flow pattern maps and flow visualization for non-boiling two-phase flow in horizontal and slightly inclined pipe," *Heat Transfer Engineering,* vol. 28, pp. 525-540, 2007.

[58] C. C. Tang and A. J. Ghajar, "Validation of a general heat transfer correlation for non-boiling two-phase flow with different flow patterns and pipe inclination angles," in *Proceedings of the 2007 ASME-JSME Thermal Engineering Summer Heat Transfer Conference*, Vancouver, BC, Canada, 2007.

[59] A. J. Ghajar, J. Kim, and C. Tang, "Two-phase flow heat transfer measurements and correlation for the entire flow map in horizontal pipes," in *Proceedings of the 13th International Heat Transfer Conference*, Sydney, Australia, 2006.

[60] A. J. Ghajar and J. Kim, "Calculation of local inside-wall convective heat transfer parameters from measurements of local outside-wall temperatures along an electrically heated circular tube," in *Heat transfer calculations*, M. Kutz, Ed. New York: McGraw-Hill, 2006, pp. 23.3-23.27.

[61] D. Kim and A. J. Ghajar, "Heat transfer measurements and correlations for air-water flow of different flow patterns in a horizontal pipe," *Experimental Thermal and Fluid Science,* vol. 25, pp. 659-676, 2002.

[62] W. B. Durant, "Heat transfer measurement of annular two-phase flow in horizontal and a slightly upward inclined tube," M.S. thesis, Oklahoma State University, Stillwater, Oklahoma, 2003.

[63] S. J. Kline and F. A. McClintock, "Describing uncertainties in single-sample experiments," *Mechanical Engineering,* vol. 75, pp. 3-8, 1953.

[64] W. L. Cook, "An experimental apparatus for measurement of pressure drop, void fraction and non-boiling two-phase heat transfer and flow visualization in pipes for all inclinations," M.S. thesis, Oklahoma State University, Stillwater, Oklahoma, 2008.

[65] Y. Taitel and A. E. Dukler, "A model for predicting flow regime transitions in horizontal and near horizontal gas-liquid flow," *AIChE Journal,* vol. 22, pp. 47-55, 1976.

[66] D. Barnea, O. Shoham, Y. Taitel, and A. E. Dukler, "Flow pattern transition for gas-liquid flow in horizontal and inclined pipes. Comparison of experimental data with theory," *International Journal of Multiphase Flow,* vol. 6, pp. 217-225, 1980.

[67] J. M. Mandhane, G. A. Gregory, and K. Aziz, "A flow pattern map for gas-liquid flow in horizontal pipes," *International Journal of Multiphase Flow,* vol. 1, pp. 537-553, 1974.

[68] G. B. Wallis, "Flooding velocities for air and water in vertical tubes," Report AEEW-R123, UKAEA, Harwell, UK, 1961.

[69] K. W. McQuillan and P. B. Whalley, "Flow patterns in vertical two-phase flow," *International Journal of Multiphase Flow,* vol. 11, pp. 161-175, 1985.

[70] F. A. Franca, A. C. Bannwart, R. M. T. Camargo, and M. A. L. Gonçalves, "Mechanistic modeling of the convective heat transfer coefficient in gas-liquid intermittent flows," *Heat Transfer Engineering,* vol. 29, pp. 984-998, 2008.

[71] W. R. Dorresteijn, "Experimental study of heat transfer in upward and downward two-phase flow of air and oil through 70-mm tubes," in *Proceedings of the 4th International Heat Transfer Conference*, Paris & Versailles, France, 1970.

[72] G. H. Abdul-Majeed and N. B. Abu Al-Soof, "Estimation of gas–oil surface tension," *Journal of Petroleum Science and Engineering,* vol. 27, pp. 197-200, 2000.

[73] L. C. Witte, W. S. Bousman, and L. B. Fore, "Studies of two-phase flow dynamics and heat transfer at reduced gravity conditions," NASA Contractor Report 198459, NASA Lewis Research Center, Cleveland, Ohio, USA, 1996.

[74] P. V. Godbole, "Study of flow patterns and void fraction in vertical upward two-phase flow," M.S. thesis, Oklahoma State University, Stillwater, Oklahoma, 2009.